ORIGINAL ARTICLES

PHOTODYNAMIC THERAPY FOR VULVAR LEUKOPLAKIA

Artemyeva T.P., Tzerkovsky D.A.
N.N. Alexandrov National Cancer Center of Belarus, Minsk, Belarus

Abstract

The aim of study is to evaluate the tolerability and effectiveness of photodynamic therapy as an organ-preserving treatment in patients with vulvar leukoplakia. 50 patients with a verified diagnosis of «vulvar leukoplakia» were included in the study. The age varied from 27 to 74 years. The method of treatment assumed the use of the photosensitizer photolon (RUE «Belmedpreparaty», Belarus) administered intravenously in doses of 1.8–2.5 mg/kg. Photoirradiation of pathological foci was carried out 2.5–3 hours after intravenous injection of photolon® using a semiconductor laser «UPL PDT» (LEMT, Belarus, λ=661 nm) at exposure doses from 30 to 100 J/cm^2 with a power density of 100–170 mW/cm^2. The treatment was performed under medical anesthesia. The results of treatment were evaluated using clinical data. Adverse reactions and complications after the introduction of the photosensitizer and photoirradiation have not been observed. Complete clinical regression of the treated pathological foci was noted in 100% of cases with a follow-up observation 1 month after the treatment. At follow-up after 3 months, local recurrences of the disease were detected in 4 cases, which were successfully treated with repeated photodynamic therapy sessions. The percentage of complete regressions was 92%, partial – 8%. The obtained results allow judging on the possibility of using photodynamic therapy in the treatment of patients with vulvar leukoplakia, which allows to preserve the organ and obtain a satisfactory functional and cosmetic result.
Key words: photodynamic therapy, photosensitizer, photolon, vulvar leukoplakia.

For citations: Artemyeva T.P., Tzerkovsky D.A. Photodynamic therapy for vulvar leukoplakia, *Biomedical Photonics*, 2018, vol. 7, no. 4, pp. 4–10. (in Russ.) doi: 10.24931/2413–9432–2018–7–4–4–10.

Contacts: Tzerkovsky D.A., tzerkovsky@mail.ru

ФОТОДИНАМИЧЕСКАЯ ТЕРАПИЯ ПРИ ЛЕЙКОПЛАКИИ ВУЛЬВЫ

Т.П. Артемьева, Д.А. Церковский
Республиканский научно-практический центр онкологии и медицинской радиологии им. Н.Н. Александрова, Минск, Беларусь

Резюме

Целью данной работы была оценка переносимости и эффективности фотодинамической терапии как органосохраняющего метода лечения у пациенток с лейкоплакией вульвы. В исследование было включено 50 пациенток с верифицированным диагнозом лейкоплакия вульвы. Возраст женщин варьировал от 27 до 74 лет. Метод лечения предполагал использование фотосенсибилизатора фотолон (РУП «Белмедпрепараты», Беларусь), который вводили внутривенно в дозах 1,8-2,5 мг/кг. Облучение патологических очагов осуществляли через 2,5–3 ч после внутривенного введения фотолона с помощью полупроводникового лазера «УПЛ ФДТ» («LEMT», Беларусь, λ=661 нм) в дозах от 30 до 100 Дж/см^2 с плотностью мощности излучения 100–170 мВт/см^2. Лечение осуществляли под медикаментозным обезболиванием. Результаты лечения оценивали по клиническим данным. Нежелательных реакций после введения фотосенсибилизатора и дальнейшего облучения зарегистрировано не было. Полная клиническая регрессия пролеченных патологических очагов отмечена в 100% случаев при контрольном наблюдении через 1 мес после проведенного лечения. При контрольном наблюдении через 3 мес у 4 пациенток выявлены локальные очаги продолженного роста опухоли, которые были успешно пролечены с помощью повторного курса фотодинамической терапии. Частота полных регрессий составила 92%, частичных – 8%. Полученные результаты позволяют судить о возможности применения фотодинамической терапии в лечении пациенток с лейкоплакией вульвы с сохранением целостности органа при получении удовлетворительного функционального и косметического результата.

Ключевые слова: фотодинамическая терапия, фотосенсибилизатор, фотолон, лейкоплакия вульвы.

Для цитирования: Артемьева Т.П., Церковский Д.А. Фотодинамическая терапия при лейкоплакии вульвы // Biomedical Photonics. – 2018 – Т. 7, № 4. – С. 4–10. doi: 10.24931/2413–9432–2018–7–4–4–10.

Контакты: Церковский Д.А., tzerkovsky@mail.ru

Introduction

In the last decade, an increasing number of patients with dystrophic diseases of the vulva (DDV) has been observed, occupying from 1% to 10% in the structure of gynecological pathology [1]. These diseases defined as «neurodystrophic diseases» include lichen sclerosus (lichen, kraurosis), squamous hyperplasia (leukoplakia) and vulvar intraepithelial neoplasia (VIN) of the vulva) [2]. Leukoplakia of the vulva (LV) is a main manifestation of the squamous hyperplasia, which is a DDV involving non-keratinized stratified squamous epithelium. In the epidemiological structure of benign lesions of the vulva, over 50% of cases are squamous hyperplasia, 25% of cases are lichen sclerosus, and remaining 25% of cases include their association [3]. This group of diseases is also characterised by a high risk of malignancy: in the setting of kraurosis, the risk of malignancy is 9%; in the setting of VIN, it is from 6% to 18%; and when both processes are combined, the risk is 60% [4]. Thus, given the duration and severity of the disease course as well as the high probability of malignancy, the search for effective methods of treating this pathology is an urgent problem of modern medicine [5].

The main method of treating patients with DDV is a surgery. In most cases, the excision of nidi is performed; when the disease extent is significant, the vulvectomy is used. The advantage of this treatment method is a possibility of histological verification in tissues of removed nidi to estimate the risk of malignancy; the disadvantages include injuries, the risk of postoperative complications and, in some cases, poor cosmetic results. In addition, according to the literature, the rate of local recurrence after vulva surgeries is from 30% to 46% [7].

The key non-surgical methods of treating DDV are laser CO_2 coagulation and vaporization of pathological areas of the vulva with a radiation intensity of over 1,000 W/cm^2. Unlike surgical treatment, these therapeutic modalities provide a good cosmetic result, but, like surgical treatment, they do not affect etiopathogenetic mechanisms of diseases, which is the reason for the development of local recurrence in the early posttreatment period. The rate of local recurrence after laser CO_2 coagulation and vaporization ranges from 15% to 48% [8, 9].

A relevant research direction is the use of high-intensity focused ultrasound, which is characterized by high tolerability, a high rate of histologically proven complete regressions (up to 88.9%) and a long period of the remission (up to 6 months) [10].

The imiquimod immunomodulator has certain therapeutic opportunities [11]. During its use, the local recurrence rate is over 40% [12]. The use of application forms of 5-fluorouracil in the treatment of DDV features a low rate of complete regressions (up to 34%) and adverse events (burns of the 1st and 2nd degree, painful ulcers) [13].

The main reasons for the search for new methods of treating DDV are the frequent recurrence of the process, the long and persistent course of the disease, the unreasonable and ineffective use of drugs, which lead to the development of various psychosomatic disorders in patients that have an adverse effect on their body state and the deterioration in women's quality of life. The existing non-surgical therapies relieve the main symptom, itching of external genital organs, but they do not fully eliminate local morphological manifestations of the disease, do not provide durable remissions and require the long period of treatment. In addition, the long-term non-surgical treatment does not prevent malignancy of the disease.

One of the most promising directions for the treatment of DDV is photodynamic therapy (PDT). This treatment method is based on the use of a special substance – a photosensitizer (PS) – whose cytotoxicity is manifested when it is exposed to laser irradiation with a specific wavelength. The results of pre-sensitized tissue irradiation are apoptosis, autophagy and ischemic necrosis of the irradiated tissues [14].

The main PSs used for PDT of DDV are 5-aminolevulinic acid (5-ALA), chlorine derivatives and dyes [15–17]. The main researches are aimed at studying the efficiency of PDT of DDV with topical application of photosensitizing agents. However, the efficiency of treatment with topical application of the chlorine based PS is low compared to traditional methods (there is no effect in more than 30–40% of cases) [18].

The majority of published abroad clinical studies, which confirm the PDT efficiency, are devoted to the use of application forms of 5-ALA as a PS.

According to P. Hillemanns et al., PDT (with laser irradiation energy density of 100 J/cm^2, $\lambda = 635$ nm) with topical application of a 20% solution of 5-ALA in 25 patients with VIN of the 1st to 3rd degrees allowed to achieve a high rate of complete regressions (CR): for VIN of the 1st degree and monofocal and bifocal lesions of the 2nd and 3rd degrees, this value was 100%; for a multifocal form of the disease, it was 27% [15].

M. K. Fehr reported on 66% of clinical CRs and 57% of histologically proven CRs for PDT (with laser irradiation energy density of 80–125 J/cm^2, $\lambda = 635$ nm) with application of a 10% gel form of 5-ALA in 22 patients with VIN of the 2nd and 3rd degrees [19]. A. Zawislak et al. presented the experience of treating 23 patients with VIN of the 2nd and 3rd degrees using PDT (with laser irradiation energy density of 100 J/cm^2, $\lambda = 635$ nm) with a 20% solution of 5-ALA. The authors reported on 52% of clinical CRs and 38% of histological CRs [20].

The CIS countries have a considerable experience in application of PDT with chlorine based PSs (fotodi-

tazine, photolon, radahlorin) in the treatment of patients with DDV. For example, O. B. Otdelnova reported on the outcomes of treatment of 6 patients with benign vulvar diseases (lichen sclerosus of the vulva, squamous hyperplasia of the vulva). The authors used the fotoditazine as a PS (intravenous infusion at a dose of 1 mg/kg + application of 1 ml of 0.5% penetrator gel). Irradiation was performed using an «Atkus-2 » semiconductor laser with laser irradiation energy density of 100–200 J/cm^2 under topical anesthesia with a 2% lidocaine solution. The efficiency assessment was based on physical examination data and the presence of clinical symptoms of the disease (itching). During follow-up after 3 months, the therapeutic effect persisted. Itching relief was observed in 3 out of 4 patients with lichen sclerosus; data of cytological examination of scraping and vulvoscopy showed the complete cure in all patients with squamous hyperplasia. A good cosmetic result was reported in all cases. However, such an adverse event as a severe pain syndrome was observed in all patients during photoradiation, which limited the application of a therapeutic dose of irratiation to the nidi [18].

E. A. Chulkova reported on outcomes of PDT with a 20% ointment of 5-ALA in 90 patients with dystrophic and premalignant diseases of the vulva. The average radiation power was 1.5 W in the spectral range of 630±10 nm. The authors noted that PDT with the 20% ointment of 5-ALA proved to be an effective method that minimally injures the healthy vulvar tissue, which is very important for young and middle-aged patients [21].

O. V. Makarov presented the experience of treating 97 patients with DDV: lichen sclerosus of the vulva was verified in 75 (77.3%) patients, squamous hyperplasia of the vulva was verified in 18 (18.6%) patients, and mixed dystrophy was verified in 4 (4.1%) patients. PDT was performed with the fotoditazine: the PS was administered via IV infusion at a dose of 1 mg/kg (n=64) or applied topically as a 0.5% penetrator gel (n=33). Irradiation was carried out in a continuous or fractional mode with laser irradiation energy density of 100–250 J/cm^2 (λ=630 nm). The authors observed a high rate (90.6%) of CRs for intravenous administration of the PS and 78.8% of CRs for topical application. One year after the PDT session, the recurrence rate was 9.1% in the 1st group and 22.6% in the 2nd group [22].

A. Z. Khashukoeva performed PDT of 50 patients with DDV (lichen sclerosus, squamous hyperplasia, mixed dystrophy) using the fotoditazine (1mg/kg). The author reports a 94% of CRs (clinical) when using laser irradiation energy density of 100–250 J/cm^2 (λ=662 nm) [23].

The purpose of this work is to assess the efficiency, safety and cosmetic results in patients with DDV treated with PDT with the photolon PS.

Materials and methods

The study included 50 patients with the morphologically verified diagnosis of leukoplakia of the vulva. The patients were from 27 to 74 years old.

The clinical diagnosis was made on the basis of complaints, history and examination of patients, vulvoscopy and the results of the morphological (histological and/or cytological) examination of the pathologically changed tissues of the vulva.

The criteria for patient enrollment in the study of PDT were histological and cytological validation of the diagnosis, the absence of the severe comorbidity and a written consent to treatment. The treatment was carried out on an outpatient basis.

The PS was Photolon (RUE «Belmedpreparaty», Belarus), which is a complex of trisodium salt of chlorin e_6 with polyvinylpyrrolidone. The PS was dissolved in 200 ml of physiological saline and was administered via IV infusion at doses of 1.8–2.5 mg/kg-BM of the patient in a darkened room.

A PDT session was conducted 2.5–3 hours after the PS administration using a «UPL PDT» semiconductor laser («Lemt», Belarus, λ=661 nm). The radiation was supplied using a light cable equipped with a microlens («Biospec» LLC, Russia), which has a homogeneous distribution of the irradiation energy over the light spot.

The size of irradiation fields varied from 1.5 to 2 cm; the number of fields ranged from 1 to 4; the power density was from 0.1 to 0.17 W/cm^2; the light dose was from 40 to 100 J/cm^2. The duration of a PDT session varied from 10 to 30 minutes depending on the number of irradiation fields. The irradiated area always included 3–5 mm of normal tissues from the edges of the afflicted zone.

Due to particular sensitivity of the treated area, premedication with non-narcotic analgesics (Ketorolac, intramuscularly, 4 ml) was carried out 15–20 minutes before the session for the pain management.

The nidus response to the treatment was evaluated immediately after the PDT session and after 1, 7 and 30 days.

The tolerance of the treatment was estimated based on the frequency and severity of adverse events using the analysis of CTCAE criteria (version 4.0).

Antitumour effects of the PDT with photolon were assessed based on visual observation of changes in the area of treated nidi and information on the presence or absence of clinical symptoms of the disease (itching in the vulva for leukoplakia) 1 and 3 months after the treatment (WHO criteria):

- a complete regression (CR) is the absence of all signs of the disease after 100% resorption of nidi 1 month after the PDT, confirmed 3 months after the treatment;
- a partial regression (PR) is a decrease in the total size of the nidi by 50% or more with subsequent stabi-

lization established after 1 month and confirmed 3 months after the PDT session;
- lack of effect is a decrease in the total size of the nidi by less than 50%, a condition without a decrease or increase in the affected area.

Results and discussion

All patients that observed the light regime for 3–4 days after the treatment had no adverse events associated with skin phototoxicity (superficial skin burns, hypopigmentation and hyperpigmentation, face soft tissues oedema).

During the infusion of the photosensitizer, the condition of the patients was satisfactory, no adverse events were observed. No allergic reactions accompanied by major organs dysfunction (drop of blood pressure, bronchospasm, generalised urticaria, etc.) and requiring to stop infusion were recorded.

Oedema and hyperthermia of irradiated areas with nidi were observed in all patients immediately after the PDT session. A brown or black photochemical necrotic scab clearly separated from normal tissues was formed within 2-4 days. Complete epithelialization of the irradiated area was observed 4–8 weeks after the PDT.

PDT sessions were accompanied by moderate pain, which was managed with drugs (2% Ketorolac, intramuscularly, 4 ml) or by a decrease in a laser irradiation power density with an unchanged light dose. In 15 patients (30% of cases), the pain persisted for 3–7 days after the treatment (CTCAE, version 4.0; 1st and 2nd degrees). 5 patients (10% of cases) showed a slight increase in body temperature (up to +37.3–37.5°C).

Clinical signs of the complete regression were observed in all patients with leukoplakia of the vulva during the follow-up after 1 month. The CR rate was 100%. The second PDT courses were conducted due to an extensive nidi area and impossibility of their simultaneous irradiation because of the moderate pain.

Local nidi of the continued tumour growth were detected in 4 cases out of 50 (8%) during the follow-up after 3 months, which were successfully treated using another PDT course. The CR rate at this time point after the treatment was 92%, and the PR rate was 8%.

In the follow-up period of 6 months, a sustained remission of the clinical symptoms of the disease (itching in the vulva) in the treated nidi was observed, including 8% of cases where the second PDT course was conducted after the PR achievement.

As a result of the study, the following indications for PDT in patients with leukoplakia of the vulva were determined:

1. a morphologically verified diagnosis;
2. primary and recurrent forms of the disease;
3. resistance to traditional (non-surgical) methods of treatment;
4. a patient's refusal to be treated with traditional methods;
5. multiple lesions.

The main advantages of PDT are:

1. minimal toxicity for normal tissues located close to nidi;
2. the minimal risk of severe pain and other adverse events;
3. the lack of treatment resistance;
4. the possibility of repeated treatment sessions;
5. the possibility of combination with traditional methods of treatment;
6. the possibility of application when the process is advanced;
7. good cosmetic results;
8. the possibility of organ preservation treatment;
9. the relatively low price and availability of treatment.

The outcomes of the PDT with photolon are confirmed by the following clinical example.

Clinical example

Patient Ya. (outpatient card No. 5747/06), 62 years old. She was followed up with complaints of severe itching in the vulva since 2006. Leukoplakia of the vulva was diagnosed. In 2008–2010, surgeries were performed due to the main disease. The progression in the treatment area was observed since 2011. Non-surgical methods of treatment were ineffective.

The patient was referred for consultation and treatment to the Republican Research and Practice Centre of Oncology and Medical Radiology named after N. N. Aleksandrov. After the consultation with specialists and histological examination, the diagnosis was made: leukoplakia of the vulva, recurrent form. Treatment with PDT was recommended. Treatment: on November 21, 2012, the patient was given a PDT course with photolon administered intravenously at a dose of 2.5 mg/kg (200 mg) in hospital environment. Nidi in the vulva and perianal area were irradiated using a «UPL PDT» semiconductor laser (λ=661 nm) in a darkened room 3 hours after the PS administration. 3 fields of 2 cm diameter were irradiated with a light cable equipped with a microlens at a laser irradiation energy density of 50 J/cm^2, a power density of 0.1 W/cm^2 and a radiation power of 0.3 W for 9 minutes per field. The effect in the form of growing necrosis was observed by the end of the first week after the treatment.

After the release from the hospital, the woman performed non-specific therapy of the irradiated area. The completion of the epithelialization processes was recorded by the 6th week.

On February 21, 2013 (after 3 months), the significant improvement in the treatment zone and the lack of complaints were noted during the follow-up clinical examination (Fig. *c*).

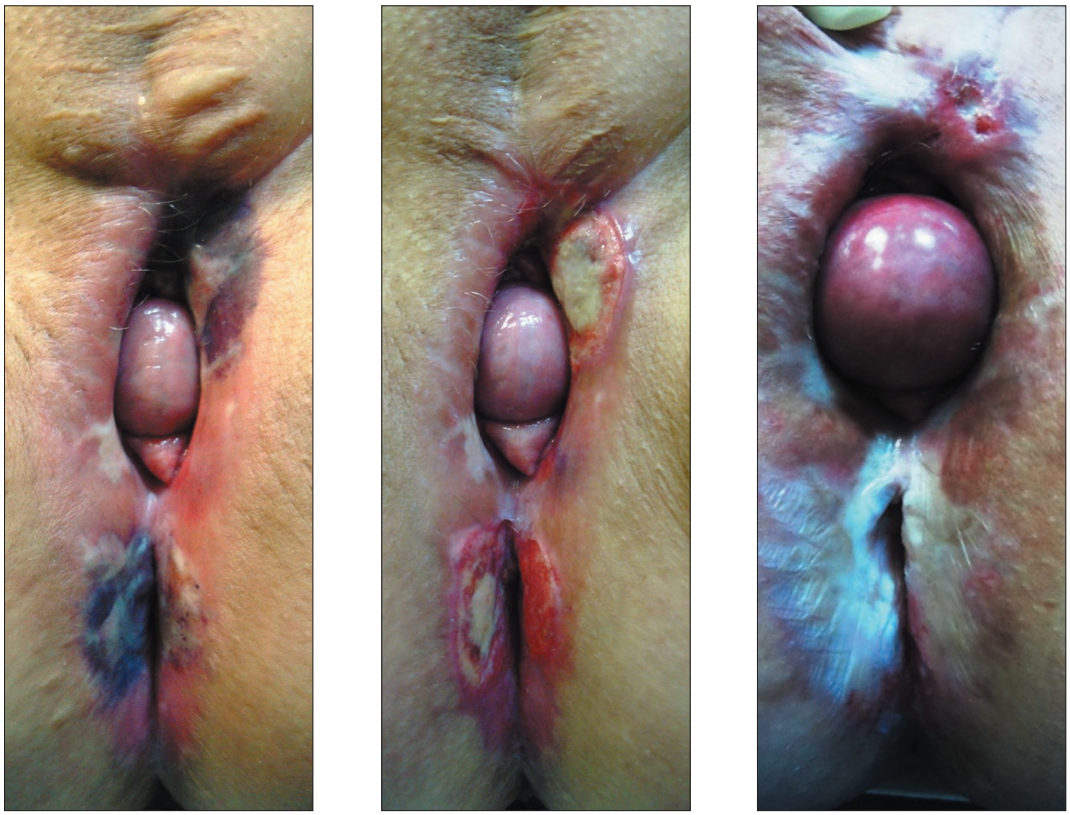

a b c

Рис. Лейкоплакия вульвы, состояние после ФДТ с фотолоном в дозе 2,5 мг/кг (плотность энергии лазерного облучения 50 Дж/см^2):
a – состояние через 24 ч после ФДТ;
b – полная регрессия через 1 мес после проведенного лечения;
c – полная регрессия через 3 мес после проведенного лечения

Fig. Vulvar leukoplakia. The state after PDT with photolon at a dose of 2.5 mg/kg and exposure dose of photoirradiation of 50 J/cm^2:
a – 24 hours after PDT
b – complete regression 1 month after the treatment;
c – complete regression 3 months after the treatment.

Conclusion

The outcomes of the clinical use of the PDT with photolon in the treatment of patients with background and premalignant diseases of the vulva presented in this study indicate its high therapeutic efficacy, minimum adverse events and good cosmetic results. During the follow-up, the complete regression of the nidi was observed in all patients. Local recurrence of the disease was detected in 8% of cases 3 months after the PDT, which was successfully treated with the second course.

It can therefore be concluded that PDT is easy to use, well tolerated, efficient and can be recommended for the treatment of dystrophic diseases and the prevention of vulvar cancer.

REFERENCES

1. Reyes M.C., Cooper K. An update on vulvar intraepithelial neoe plasia: terminology and a practical approach to diagnosis, *J. Clin. Pathol.*, 2014, vol. 67, no. 4, pp. 290–294.
2. Hendriks J., Wilkinson E.J. Vulvar lichen sclerosus: immunohisto‑ logic, *J. Reprod. Med.*, 1994, vol. 38, pp. 37–40.
3. Judson P.L., Habermann E.B., Baxter N.N., Durham S.B., Virnig B.A. Trends in the incidence of invasive and in situ vulvar carcinoma, *Obstet. Gynecol.*, 2006, vol. 107, no. 5, pp. 1018–1022.

ЛИТЕРАТУРА

1. Reyes M.C., Cooper K. An update on vulvar intraepithelial neoplaM sia: terminology and a practical approach to diagnosis // J. Clin. Pathol. – 2014. – Vol. 67, No. 4. – P. 290–294.
2. Hendriks J., Wilkinson E.J. Vulvar lichen sclerosus: immunohisto‑ logic // J. Reprod. Med. – 1994. – Vol. 38. – P. 37–40.
3. Judson P.L., Habermann E.B., Baxter N.N., et al. Trends in the inciо dence of invasive and in situ vulvar carcinoma // Obstet. Gynecol. – 2006. – Vol. 107, No. 5. – P. 1018–1022.

4. Kozachenko V.P. *Onkoginekologiya: rukovodstvo dlya vrachei* [Oncogynecology: a guide for doctors]. Moscow, Meditsina Publ., 2006, 560 p.
5. Rogovskaya S.I., Bebneva T.N. Leukoplakia of the cervix, vagina and vulva. Modern aspects, *Bolezni vlagalishcha i shejki matki*, 2014, no. 1, pp. 51–55. (in Russ.)
6. Gu Y., Zhu L., Li X., Jin H., Wang C. Surgical treatment of usual type vulvar intraepithelial neoplasia: a study at three academic hospitals, *Chin. Med. J. (Engl)*, 2014, vol. 127, no. 4, pp. 784–786.
7. Mahner S., Wölber L. Surgery or topical therapy for vulval intraepithelial neoplasia, *Lancet Oncol*, 2014, vol. 15, no. 12, pp. 1287–1288.
8. Hillemanns P., Wang X., Staehle S., Michels W., Dannecker C. Evaluation of different treatment modalities for vulvar intraepithelial neoplasia (VIN): CO2 laser vaporization, photodynamic therapy, excision and vulvectomy, *Gynecol. Oncol.*, 2005, vol. 100, no. 2, pp. 271–275.
9. Kushnir C.L., Fleury A.C., Hill M.C., Silver D.F., Spirtos N.M. The use of argon beam coagulation in treating vulvar intraepithelial neoplasia III: a retrospective review, *Gynecol. Oncol.*, 2013, vol. 131, no. 2, pp. 386–388.
10. Jia Y., Wu J., Xu M., Tang L., Li C. Clinical responses to focused ultrasound applied to women with vulvar intraepithelial neoplasia, *J. Ultrasound Med.*, 2014, vol. 33, no. 11, pp. 1903–1908.
11. Kim J.M., Lee H.J., Kim S.H., Kim H.S., Ko H.C. Efficacy of 5% imiquimod cream on vulvar intraepithelial neoplasia in Korea: pilot study, *Ann. Dermatol.*, 2015, vol. 27, no. 1, pp. 66–70.
12. Westermann C., Fischer A., Clad A. Treatment of vulvar intraepithelial neoplasia with topical 5% imiquimod cream, *Int. J. Gynaecol. Obstet.*, 2013, vol. 120, no. 3, pp. 266–270.
13. Preti M., Van Seters M., Sideri M., Van Beurden M. Squamous vulvar intraepithelial neoplasia, *Clin. Obstet. Gynecol.*, 2005, vol. 48, no. 4, pp. 845–861.
14. Dougherty T.J., Gomer C.J., Henderson B.W., Jori G., Kessel D. Photodynamic Therapy, *J. Nat. Cancer Ins.*, 1998, vol. 90, no. 12, pp. 889–905.
15. Hillemanns P., Untch M., Dannecker C., Baumgartner R., Stepp H. Photodynamic therapy of vulvar intraepithelial neoplasia using 5-aminolevulinic acid, *Int J Cancer*, 2000, vol. 85(5), pp. 649–653.
16. Ignatova T.P., Rusakevich P.S., Rogov Yu.I. Clinical and morphological aspects of dystrophic diseases of the vulva in the process of photodynamic therapy with methylene blue, *Onkol. zhurn.*, 2008, vol. 2, no. 2, pp. 105–125. (in Russ.)
17. Rusakevich P.S., Grishanovich R.V., Plavskij V.Yu. Possibilities of using photodynamic therapy with local application of photosensitizers in neurodystrophic diseases of vulva, cervical ectopia and metaplasia, Onkol. Zhurn., 2010, vol. 4, no. 1(13), pp. 47–53. (in Russ.)
18. Otdel'nova O.B., Hashukoeva A.Z., Ibragimova M.I. Possibilities of photodynamic therapy using fotoditazin photosensitizer in the treatment of gynecological diseases, *Ros. bioter. zhurn.*, 2008, vol. 7, no. 4, pp. 47–52. (in Russ.)
19. Fehr M.K., Hornung R., Degen A., Schwarz V.A., Fink D. Photodynamic therapy of vulvar and vaginal condyloma and intraepithelial neoplasia using topically applied 5-aminolevulinic acid, *Lasers Surg. Med.*, 2002, vol. 30, no. 4, pp. 273–279.
20. Zawislak A., Donnelly R.F., McCluggage W.G., Price J.H., McClelland H.R. Clinical and immunohistochemical assessment of vulval intraepithelial neoplasia following photodynamic therapy using a novel bioadhesive patch-type system loaded with 5-aminolevulinic acid, *Photodiagnosis Photodyn. Ther.*, 2009, vol. 6, no. 1, pp. 28–40.
21. Chulkova E.A., Makarov I.O., Sokolov V.V. Modern aspects of fluorescent diagnostics and photodynamic therapy with 5-aminolevulinic acid (Alasens) for background and precancerous diseases of the vulva, *Zhurnal akusherstva i zhenskikh boleznei*, 2009, vol. LVIII, no. 5, pp. 91–92. (in Russ.)

4. Козаченко В.П. Онкогинекология: руководство для врачей. – М.: Медицина, 2006. – 560 с.
5. Роговская С.И., Бебнева Т.Н. Лейкоплакия шейки матки, влагалища и вульвы. Современные аспекты // Болезни влагалища и шейки матки. – 2014. – № 1. – С. 51–55.
6. Gu Y., Zhu L., Li X., et al. Surgical treatment of usual type vulvar intraepithelial neoplasia: a study at three academic hospitals // Chin. Med. J. (Engl). – 2014. – Vol. 127, No. 4. – P. 784–786.
7. Mahner S., Wölber L. Surgery or topical therapy for vulval intraepithelial neoplasia // Lancet Oncol. – 2014. – Vol. 15, No. 12. – P. 1287–1288.
8. Hillemanns P., Wang X., Staehle S., et al. Evaluation of different treatment modalities for vulvar intraepithelial neoplasia (VIN): CO_2 laser vaporization, photodynamic therapy, excision and vulvectomy // Gynecol. Oncol. – 2005. – Vol. 100, No. 2. – P. 271–275.
9. Kushnir C.L., Fleury A.C., Hill M.C., et al. The use of argon beam coagulation in treating vulvar intraepithelial neoplasia III: a retrospective review // Gynecol. Oncol. – 2013. – Vol. 131, No. 2. – P. 386–388.
10. Jia Y., Wu J., Xu M., et al. Clinical responses to focused ultrasound applied to women with vulvar intraepithelial neoplasia // J. Ultrasound Med. – 2014. – Vol. 33, No. 11. – P. 1903–1908.
11. Kim J.M., Lee H.J., Kim S.H., et al. Efficacy of 5% imiquimod cream on vulvar intraepithelial neoplasia in Korea: pilot study // Ann. Dermatol. – 2015. – Vol. 27, No. 1. – P. 66–70.
12. Westermann C., Fischer A., Clad A. Treatment of vulvar intraepithelial neoplasia with topical 5% imiquimod cream // Int. J. Gynaecol. Obstet. – 2013. – Vol. 120, No. 3. – P. 266–270.
13. Preti M., Van Seters M., Sideri M., Van Beurden M. Squamous vulvar intraepithelial neoplasia // Clin. Obstet. Gynecol. – 2005. – Vol. 48, No. 4. – P. 845–861.
14. Dougherty T.J., Gomer C.J., Henderson B.W., et al. Photodynamic Therapy // J. Nat. Cancer Ins. – 1998. – Vol. 90, No. 12. – P. 889–905.
15. Hillemanns P., Untch M., Dannecker C., et al. Photodynamic therapy of vulvar intraepithelial neoplasia using 5-aminolevulinic acid // Int J Cancer. – 2000. – Vol. 85(5). – P. 649–653.
16. Игнатова Т.П., Русакевич П.С., Рогов Ю.И. Клинико-морфологические аспекты при дистрофических заболеваниях вульвы в процессе фотодинамической терапии с метиленовым синим // Онкол. журн. – 2008. – Т. 2, № 2. – С. 105–125.
17. Русакевич П.С., Гришанович Р.В., Плавский В.Ю. Возможности применения фотодинамической терапии с местным применением фотосенсибилизаторов при нейродистрофических заболеваниях вульвы, цервикальной эктопии и метаплазии // Онкол. Журн. – 2010. – Т. 4, № 1(13). – С. 47–53.
18. Отдельнова О.Б., Хашукоева А.З., Ибрагимова М.И. Возможности фотодинамической терапии с использованием фотосенсибилизатора фотодитазин в лечении гинекологических заболеваний // Рос. биотер. журн. – 2008. –Т. 7, № 4. – С. 47–52.
19. Fehr M.K., Hornung R., Degen A., et al. Photodynamic therapy of vulvar and vaginal condyloma and intraepithelial neoplasia using topically applied 5-aminolevulinic acid // Lasers Surg. Med. – 2002. – Vol. 30, No. 4. – P. 273–279.
20. Zawislak A., Donnelly R.F., McCluggage W.G., et al. Clinical and immunohistochemical assessment of vulval intraepithelial neoplasia following photodynamic therapy using a novel bioadhesive patch-type system loaded with 5-aminolevulinic acid // Photodiagnosis Photodyn. Ther. – 2009. – Vol. 6, No. 1. – P. 28–40.
21. Чулкова Е.А., Макаров И.О., Соколов В.В. Современные аспекты флуоресцентной диагностики и фотодинамической терапии с 5-аминолевулиновой кислотой («Аласенс») при фоновых и предраковых заболеваниях вульвы // Журнал акушерства и женских болезней. – 2009. – Т. LVIII, Вып. 5. – С. 91–92.

22. Makarov O.V., Khashukoeva A.Z., Kupeeva E.S., Khlynova S.A., Sukhova T.N. Treatment of dystrophic diseases of the vulva using photodynamic therapy, *Vestnik RGMU*, 2014, no. 4, pp. 49–52. (in Russ.)
23. Khashukoeva A.Z., Kupeeva E.S., Otdelnova O.B. Photodynamic therapy in the treatment of dystrophic diseases of the vulva, *Fotodinamicheskaya terapiya i fotodiagnostika*, 2012, no. 1, pp. 31. (in Russ.)

22. Макаров О.В., Хашукоева А.З., Купеева Е.С. и др. Лечение дистрофических заболеваний вульвы методом фотодинамической терапии // Вестник РГМУ. – 2014. – № 4. – С. 49–52.
23. Хашукоева А.З., Купеева Е.С., Отдельнова О.Б. Фотодинамическая терапия в лечении дистрофических заболеваний вульвы // Фотодинамическая терапия и фотодиагностика. – 2012. – № 1. – С. 31.

CYTOLOGICAL EFFECTS IN LYMPH NODES OF ABDOMINAL LYMPHODISSECTION ZONE AFTER INTRAOPERATIVE PHOTODYNAMIC THERAPY OF GASTROINTESTINAL CANCERS

Kravtsov V.Yu.[1,2], Pirozhenko E.S.[1], Pavelec K.V.[2,3,4], Protchenkov M.A.[2,4], Drozd U.A.[3]
[1]Military Medical Academy of S.M. Kirov, Saint-Petersburg, Russia
[2]North-Western State Medical University named after I.I. Mechnikov, Saint-Petersburg, Russia
[3]Saint-Petersburg State Pediatric Medical University, Saint-Petersburg, Russia
[4]Mariinsky hospital, St-Petersburg, Russia

Abstract

Cytological studies on lymph nodes of abdominal lymphodissection zone after local intraoperative photodynamic therapy (IOPDT) of gastrointestinal cancers were carried out. As a result of the PDT, the metastatic cells are destroyed, their cytoplasmic membranes and the cytoplasm disappears, leaving behind interphase nuclei ("naked nuclei") ($p<0,0001$). Cytological confirmation of apoptosis (the presence of apoptotic bodies) in metastatic lymph nodes after IOPDT sessions on the lymph nodes of the abdominal lymphodissection zone is also presented.

Keywords: photodynamic therapy, cytopathology, interphase nucleus, apoptosis, radachlorin, fotoditazin.

For citations: Kravtsov V.Yu., Pirozhenko E.S., Pavelec K.V., Protchenkov M.A., Drozd U.A. Cytological effects in lymph nodes of abdominal lymphodissection zone after intraoperative photodynamic therapy of gastrointestinal cancers, *Biomedical photonics*, 2018, vol. 7, no. 4, pp. 11–15. (in Russ.) doi: 10.24931/2413–9432–2018–7–4–11–15.

Contacts: Kravtsov V.Yu., e-mail: kvyspb@mail.ru

ЦИТОЛОГИЧЕСКИЕ ЭФФЕКТЫ В ЛИМФАТИЧЕСКИХ УЗЛАХ ЗОНЫ АБДОМИНАЛЬНОЙ ЛИМФОДИССЕКЦИИ ПОСЛЕ ИНТРАОПЕРАЦИОННОЙ ФОТОДИНАМИЧЕСКОЙ ТЕРАПИИ ПРИ ЗЛОКАЧЕСТВЕННЫХ НОВООБРАЗОВАНИЯХ ЖЕЛУДОЧНО-КИШЕЧНОГО ТРАКТА

В.Ю. Кравцов[1,2], Е.С. Пироженко[1], К.В. Павелец[2,3,4], М.А. Протченков[2,4], У.А. Дрозд[3]
[1]Военно-медицинская академия им. С.М. Кирова, Санкт-Петербург, Россия
[2]Северо-Западный государственный медицинский университет имени И.И. Мечникова, Санкт-Петербург, Россия
[3]Санкт-Петербургский государственный педиатрический медицинский университет, Санкт-Петербург, Россия
[4]Городская Мариинская больница, Санкт-Петербург, Россия

Резюме

Проведены цитологические исследования материала лимфатических узлов зоны абдоминальной лимфодиссекции после интраоперационной фотодинамической терапии (ИОФДТ) при злокачественных новообразованиях желудочно-кишечного тракта. Установлено, что в результате проведения ФДТ клетки метастатических опухолей разрушаются с исчезновением цитоплазматической мембраны и цитоплазмы, при этом остаются только интерфазные ядра («голые ядра») ($p<0,0001$). Также представлено цитологическое подтверждение апоптоза (наличие апоптотических телец) в лимфатических узлах с метастазами после курсов ИОФДТ в лимфатических узлах зоны абдоминальной лимфодиссекции.

Ключевые слова: фотодинамическая терапия, цитопатология, интерфазные ядра, апоптоз, радахлорин, фотодитазин.

Для цитирования: Кравцов В.Ю., Пироженко Е.С., Павелец К.В., Протченков М.А., Дрозд У.А. Цитологические эффекты в лимфатических узлах зоны абдоминальной лимфодиссекции после интраоперационной фотодинамической терапии при злокачественных новообразованиях желудочно-кишечного тракта // Biomedical photonics. – 2018. – Т. 7, № 4. – С. 11–15. doi: 10.24931/2413–9432–2018–7–4–11–15.

Контакты: Кравцов В.Ю., e-mail: kvyspb@mail.ru

Introduction

A study of lymph nodes of the zone of abdominal lymph node dissection performed after intraoperative photodynamic therapy (IOPDT) with the radahlorin or fotoditazine photosensitizer (PS) to detect apoptosis in case of malignant tumours of the gastrointestinal tract was described in the previously published article. Using DNA electrophoresis, it was proved that apoptosis after PDT is induced in lymph nodes affected by metastases and does not occur in intact lymph nodes ($p < 0.01$). This fact indicates the selective ability of PDT to cause the death of malignant cells [1].

In this study, cytologic preparations used in the previous stages to detect metastases were analyzed again under immersion. The purpose of this retrospective study was to search for cytological manifestations of apoptotic (apoptotic bodies) and necrotic (cytonecrosis, phagocytic infiltration) processes in populations of metastatic lymph node cells induced by PDT.

Materials and methods

The groups of examined patients and their diagnoses, the procedure for PDT sessions and obtaining cytologic preparations from lymph nodes were described in detail in the previously published article [1].

Cytological examinations were performed on preparations obtained by imprinting of irradiated and non-irradiated parts of lymph nodes on glasses.

The preparations were Romanowsky-Giemsa stained and microscoped under immersion (x1000) in transmitted light. The frequency of ill-defined cells (nuclei) was found by counting 500–1000 tumour cells and expressed as a percentage.

Statistical processing of data was performed with nonparametric techniques (Wilcoxon-Mann-Whitney U test) using the Statistica 13.3 software package.

Results

The findings of the study of 40 lymph nodes obtained by the above mentioned method were set forth in the previous article. Metastatic cells were detected in 23 lymph nodes; no metastatic cells were detected in 17 of them. Using DNA electrophoresis, apoptosis (apoptotic ladders) was detected in 17 of 23 lymph nodes affected by metastases [1].

Now we can confirm that cytological examinations in imprint smears performed in the same 17 lymph nodes revealed apoptotic bodies (Fig. 1).

During microscopy under immersion, a sharp contrast in the frequency of the so-called «bare nuclei» (BN) of malignant metastatic cells was found between irradiated and non-irradiated halves of lymph nodes. This phenomenon was observed both in squamous and glandular malignant tumours. In both cases, the nuclei had clear, even boundaries; the nature of staining and chromatin structure corresponded to intact cells with a cytoplasm and membrane (Fig. 2a). The observed «bare nuclei» were both located separately (Fig. 2b) and associated in the form of bunches of grapes, which probably corresponded to the induction of «bare nuclei» simultaneously and immediately after irradiation of metastatic cell complexes (Fig. 2).

Analyses of the frequency of BN of metastatic cells in irradiated and non-irradiated lymph nodes with metastases in 15 patients with adenocarcinoma and 19 patients with squamous cell carcinoma were performed in

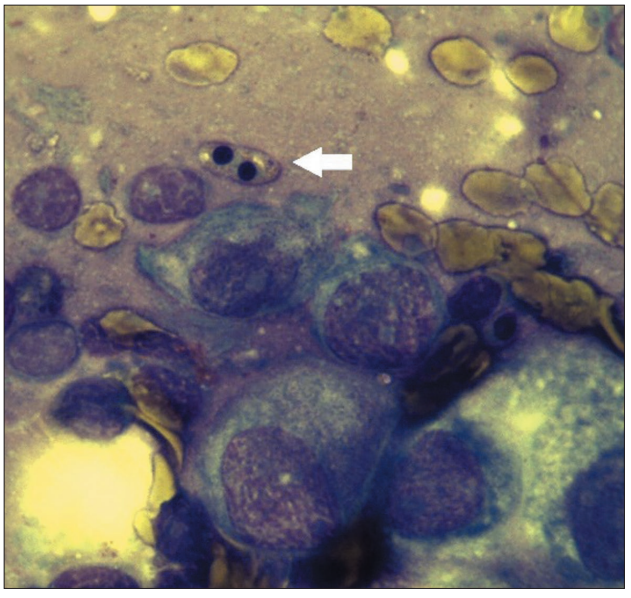

Рис. 1. Апоптотические тельца метастатических клеток аденокарциномы желудка в лимфатических узлах после проведения сеанса ФДТ
Fig. 1. Apoptotic bodies of metastatic cells in the lymph nodes of adenocarcinoma of stoma after PDT session

the STATISTICA programme and presented in bar graphs (Fig. 3, 4).

Obviously, the effect of IOPDT significantly increases the number of «bare nuclei» ($p<0.0001$, Wilcoxon-Mann-Whitney U test).

Thus, we obtained cytological validation of apoptosis (the presence of apoptotic bodies) in lymph nodes with metastases after IOPDT, which we had previously detected using DNA electrophoresis [1]. Moreover, in our opinion, the most important thing revealed during this study was the «under the beam» effect manifested in the form of induction of «bare nuclei» of metastatic cells after PDT.

Cytological evidence of the death of tumour cells by apoptosis and necrosis allows us to conclude that IOPDT can increase the ablasticity of surgical interventions and improve the oncological outcomes of resections for locally advanced malignant tumours of the gastrointestinal tract.

Discussion

Obviously, the observed PDT-induced «bare nuclei» could only occur when the cells were damaged in the cytoplasm (lysosomes, mitochondria, Goldgi complex and endoplasmic reticulum) and cytoplasmic membrane, but not inside or even on the surface of the cell nucleus. Nucleus intactness during PDT was observed in the study of the subcellular localization of Foscan in the MCF-7 human adenocarcinoma line by M. H. Teiten et al. [2]. Using confocal microscopy and microspectrofluorimetry, the authors showed that this PS slightly accumulates in lysosomes and mitochondria and is mainly localized in the Goldgi complex and endoplasmic reticulum, without affecting the nucleus. According to the study by A. P. Castano et al., the PSs are localized in mitochondria, lysosomes, endoplasmic reticulum, Goldgi complex and plasmalemma [3]. S. Farrakhova et al. studied the localization of chlorine e_6 and its dimethyl ether in HT29 cells of the human adenocarcinoma and found that these photosensitizers are mainly distributed in the plasmalemma and cytoplasm of cells and scarcely accumulate in the area of cell nucleus localization [4].

However, L. S. Fontana et al. obtained ambiguous results when studying the intracellular localization of the fotoditazine PS in the 9L/LacZ glioblastoma cell line. Fluorescence microscopy showed diffuse uptake of the PS in the whole cell, but it was impossible to say for certain whether the PS accumulates in the nucleus. The author himself believes that the false-positive result could be related to the association of fotoditazin with the nuclear membrane [5]. L. S. Fontana also faced the phenomenon of induction of «bare nuclei» and gave them a description that is entirely congruent with the one we had previously presented [6]. The very first report on the induction of BN during PDT, which we managed to find in the PubMed search engine, is given in the Chinese journal by the researcher Y. T. Zhou et al. [7]. It should be noted that «bare nuclei» of L. S. Fontana and «bare nuclei» of Y. T. Zhou were induced by PDT in cell cultures *in vitro*.

Despite the fact that L. S. Fontana's data indicate the association of the PS with the nucleus, it is obvious that the presence of radahlorin on the nucleus surface is still insufficient for its destruction after photoactivation.

The damage radius of the activated PS is relatively small on a subcellular scale [2, 3, 8, 9]. High reactivity and a short half-life of the singlet oxygen and hydroxyl radicals directly affect only molecules and structures that are located close to the area of their production (PS localization area). The half-life of singlet oxygen in biosystems is < 40 ns, therefore the radius of action of singlet oxygen is

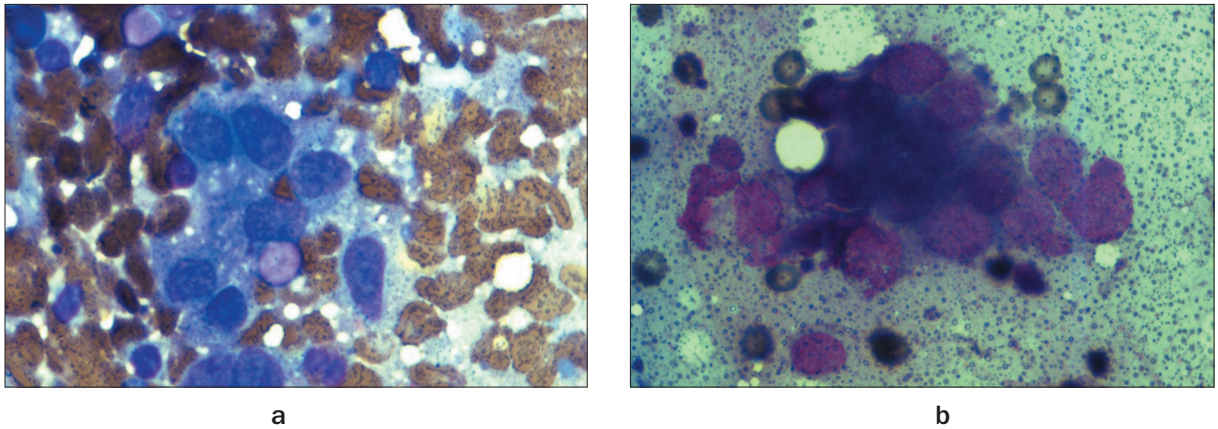

Рис. 2. Мазки-отпечатки метастатических клеток в лимфатическом узле 9А зоны абдоминальной лимфодиссекции до облучения (a) и после завершения (b) сеанса интраоперационной фотодинамической терапии, выполняемой аппаратом «Фара-2» в течении 20 мин (окрашивание азур-эозином по Романовскому, увеличение: x1000)
Fig. 2. Imprint smear of metastatic cells in the lymph node (9A) of the abdominal lymph node dissection zone before (a) and after (b) intraoperative PDT session carried out using «Fara-2» device for 20 minutes (staining with azur-eosin by Romanovsky, magnification: x1000).

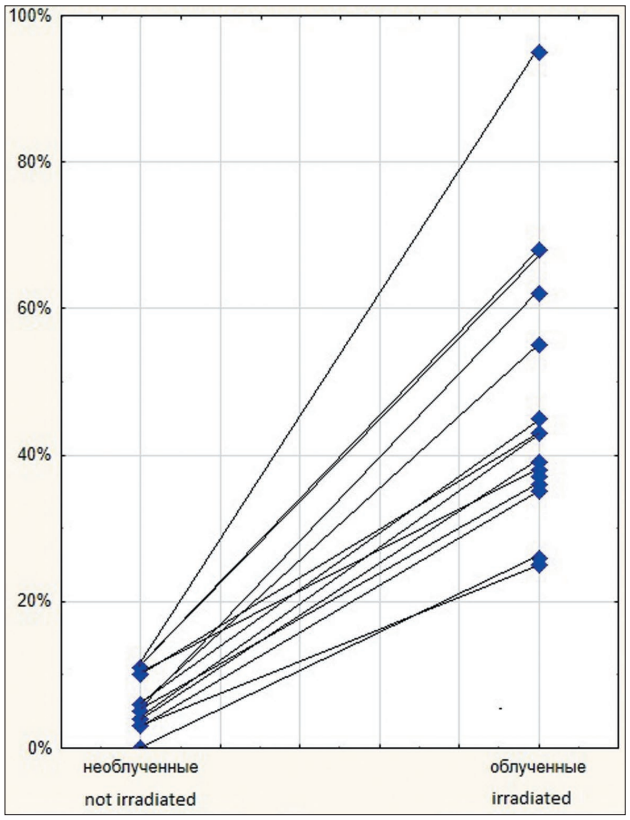

Рис. 3. Распределение половин лимфатических узлов по показателю «частота встречаемости "голых ядер"» при железистом раке
Fig. 3. Distribution of halves of lymph nodes according to the "frequency of occurrence of "naked nuclei" with glandular cancer

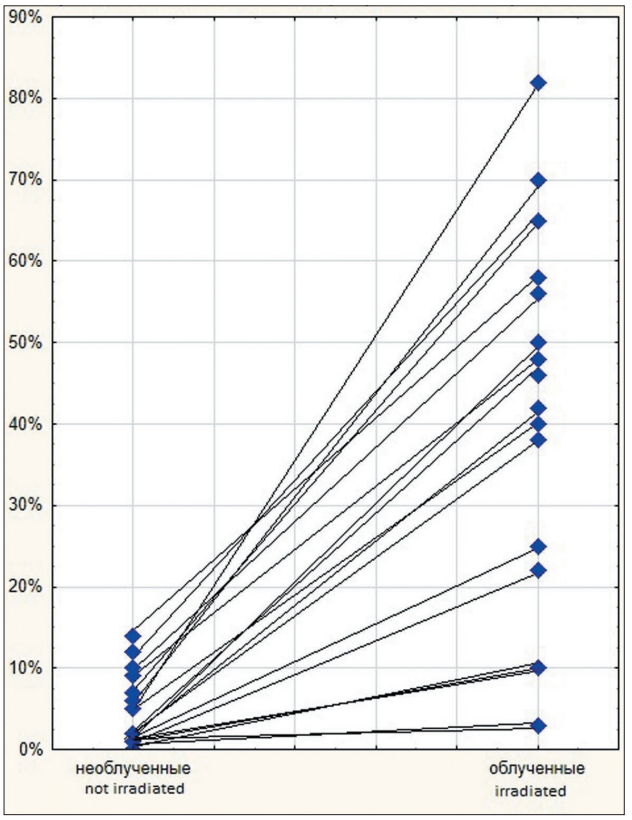

Рис. 4. Распределение половин лимфатических узлов по показателю «частота встречаемости "голых ядер"» при плоскоклеточном раке
Fig. 4. Distribution of halves of lymph nodes according to the "frequency of occurrence of "naked nuclei" with squamous cell carcinoma

about 20 nm [2], while the thickness of the nuclear membrane (34–74 nm) is greater by several fold than the possible damage radius of the photosensitizer. That is why the nucleus generally holds its shape after PDT.

Conclusion

IOPDT conducted in patients with malignant tumours of the gastrointestinal tract causes the «under the beam» effect, which is manifested in the induction of «bare nuclei» of metastatic cells of abdominal lymph nodes of the lymph node dissection area. During the study, cytological validation of apoptosis (the presence of apoptotic bodies) in lymph nodes with metastases after PDT sessions in the lymph nodes of the abdominal lymph node dissection area was presented. The use of IOPDT in a clinical setting increases the ablasticity of surgeries and oncological effectiveness of surgical treatment of locally advanced forms of the gastrointestinal cancer.

REFERENCES

1. Pavelec K.V., Orel V.I., Kravtsov V.Y., Protchencov M.A., Dysin A.V., Drozd U.A., Kuzmina T.I., Kostina U.D., Pavelec M.K., Rusanov D.S., Lacko E.F. Apoptosis in the lymph nodes of the abdominal lymphodissection zone after local intraoperative photodynamic therapy of gastrointestinal cancers, *Biomedical Photonics*, 2017, vol. 6, no. 3, pp. 39–44. (In Russian)
2. Teiten M.H., Bezdetnaya L., Morliere P., Santus R., Guillemin F. Endoplasmic reticulum and Golgi apparatus are the preferential sites of Foscan localisation in cultured tumour cells, *Br J Cancer*, 2003, vol. 88, pp. 146–152.
3. Castano A.P., Demidova T.N., Hamblin M.R. Mechanisms in photodynamic therapy: part one—-photosensitizers, photochemish

ЛИТЕРАТУРА

1. Павелец К.В., Орёл В.И., Кравцов В.Ю. и др. Изучение апоптоза в лимфатических узлах зоны абдоминальной лимфодиссекции после интраоперационной фотодинамической терапии при злокачественых новообразованиях желудочно-кишечного тракта // Biomedical Photonics. – 2017. – Т. 6, № 3. – С. 39–44.
2. Teiten M.H., Bezdetnaya L., Morliere P., et al. Endoplasmic reticulum and Golgi apparatus are the preferential sites of Foscan localisation in cultured tumour cells // Br J Cancer. – 2003. – Vol. 88. – P. 146–152.
3. Castano A.P., Demidova T.N., Hamblin M.R. Mechanisms in photodynamic therapy: part one—-photosensitizers, photochem-

try and cellular localization, *Photodiagnosis Photodyn Ther*, 2004, vol.1, no. 4, pp. 279–293.

4. Farrahova D.S., YAkovec M.V., Loshchenov V.B., Bolotine L.N., Zorin V.P. Investigation of chlorin photosensitizers distribution in monolayer and spheroid cell cultures, *Biomedical Photonics*, 2017, vol. 6, no. 2, pp. 4–11. (In Russian)
5. Fontana L.C., Pinto J.G., Pereira A.H.C., Soares C.P., Raniero L.J., Ferreira-Strixino J. Photodithazine photodynamic effect on viability of 9L/lacZ gliosarcoma cell line, *Lasers Med Sci*, 2017, vol. 32, no. 6, pp. 1245–1252.
6. Pavelets K.V., Kravtsov V.Yu., Protchenkov M.A., Savinov I.P., Vitale eva U.A., Rusanov D.S., Fedorova P.S., Pavelets M.K., Kostina Yu.D. First experience of using intraoperative fluorescent diagnostics and photodynamic therapy in abdominal oncology, *Biomedical Photonics*, 2015, S. 1, pp. 69–70. (In Russian)
7. Zhou Y.K., Wu W.Z., Zhang L., Yang C.H., Wang Y.P. Effect of M007 mediated photodynamic therapy on proliferation of human osteosarcoma MG63 cells in vitro, *Sichuan Da Xue Xue Bao Yi Xue Ban*, 2012, vol. 43, no. 1, pp. 41–45.
8. Moan J., Berg K. The photodegradation of porphyrins in cells can be used to estimate the lifetime of singlet oxygen, *Photochem Photobiol*, 1991, vol. 53, no. 4, pp. 549–553.
9. Kessel D., Luol Y., Deng Y., Chang C.K. The Role of Subcellular Localization in Initiation of Apoptosis by Photodynamic Therapy, *Photochemistry and Photobiology*, 1997, vol. 65, no. 3, pp. 422–42

istry and cellular localization // Photodiagnosis Photodyn Ther. – 2004. – Vol.1, No. 4. – P. 279–293.

4. Фаррахова Д.С., Яковец М.В., Лощенов В.Б. и др. Исследование распределения хлориновых фотосенсибилизаторов в двухмерных и трехмерных клеточных культурах // Biomedical Photonics. – 2017. – Т. 6, № 2. – С. 4–11.
5. Fontana L.C., Pinto J.G., Pereira A.H.C., et al. Photodithazine photodynamic effect on viability of 9L/lacZ gliosarcoma cell line // Lasers Med Sci. – 2017. – Vol. 32, No. 6. – P. 1245–1252.
6. Павелец К.В., Кравцов В.Ю., Протченков М.А. и др. Первый опыт применения интраоперационной флюоресцентной диагностики и фотодинамической терапии в абдоминальной онкологии // Biomedical Photonics. – 2015. – S. 1. – С. 69–70.
7. Zhou Y.K., Wu W.Z., Zhang L., et al. Effect of M007 mediated photodynamic therapy on proliferation of human osteosarcoma MG63 cells in vitro // Sichuan Da Xue Xue Bao Yi Xue Ban. – 2012. – Vol. 43, No. 1. – P. 41–45.
8. Moan J., Berg K. The photodegradation of porphyrins in cells can be used to estimate the lifetime of singlet oxygen // Photochem Photobiol. – 1991. – Vol. 53, No. 4. – P. 549–553.
9. Kessel D., Luol Y., Deng Y., Chang C.K. The Role of Subcellular Localization in Initiation of Apoptosis by Photodynamic Therapy // Photochemistry and Photobiology. – 1997. – Vol. 65, No. 3. – P. 422–426.

ORIGINAL ARTICLES

STUDY OF PHARMACOKINETICS OF LIPOSOMAL PHOTOSENSITISER BASED ON HYDROXYALUMINIUM TETRA-3-PHENYLTHIOPHTHALOCYANINE ON MICE

Budko A.P.[1], Deichman Z.G.[1], Meerovich G.A.[2,3], Borisova L.M.[1], Meerovich I.G.[4], Lantsova A.V.[1], Kulbachevskaya N.Yu.[1]

[1]N.N. Blokhin National Medical Research Center of Oncology, Ministry of Health of Russia, Moscow, Russia of the Ministry of Health of the Russian Federation, Moscow, Russia
[2]Prokhorov General Physics Institute of the Russian Academy of Sciences, Moscow, Russia
[3]National Research Nuclear University MEPhI (Moscow Engineering Physics Institute), Moscow, Russia
[4]Bach Institute of Biochemistry, Research Center of Biotechnology of the Russian Academy of Sciences, Moscow, Russia

Abstract

The present work is devoted to the study of pharmacokinetics of infrared photosensitizer (PS) based on hydroxyaluminium tetra-3-phenylthiophthalocyanine in a sterically stabilized liposomal form. The study was carried out on adult female mice. The PS was administered once intravenously at a dose of 6 mg / kg. Evaluation of the PS accumulation dynamics in the mice tissues and organs was performed at time intervals from 5 minutes to 7 days using spectral-fluorescent method. The maximum accumulation of the PS photoactive form was recorded in lungs (32 μg / g in the interval of 5–30 minutes after introduction), liver (20.8 μg / g in the interval of 4–24 hours after introduction) and spleen (28 μg / g 4 hours after introduction). At the same time, by the end of the observation period (7 days after administration), trace amounts of the PS photoactive form were still detected in the liver and the spleen at a calculated concentration of 0.5-1 μg / g. The PS accumulated the least in muscles and skin. The fluorescent signal from the PS accumulated in skin was detectable almost immediately, and its concentration remained at the same level (1.2-1.5 μg / g) for up to 3 days of observation. In the muscles, the concentration of the PS reached 1.5 μg / g 15 minutes after administration, and then gradually decreased until 0.25 μg / g at 24 hours.

Data on the pharmacokinetics of PS in blood, basic organs and tissues of animals were obtained, pharmacokinetic parameters were calculated. 7 days after the administration, the PS concentration in the skin and muscles was below the detection limit. The studies confirmed that PEGylation of the PS liposomal form slows down the process of its capture by reticulo-endothelial system. It was shown that the PS circulates in blood and organs of mice for a long time and it completely distributes only when 4 hours pass after administration.

Keywords: photosensitizer, pharmacokinetics, fluorescence.

For citations: Budko A.P., Deichman Z.G., Meerovich G.A., Borisova L.M., Meerovich I.G., Lantsova A.V., Kulbachevskaya N.Yu. Study of pharmacokinetics of liposomal photosensitizer based on hydroxyaluminium tetra-3-phenylthiophthalocyanine on mice, *Biomedical photonics*, 2018, vol. 7, no. 4, pp. 16–22. (in Russ.) doi: 10.24931/2413–9432–2018–7–4–16–22.

Contacts: Budko A.P., e-mail: apbudko@mail.ru

ИЗУЧЕНИЕ ФАРМАКОКИНЕТИКИ ФОТОСЕНСИБИЛИЗАТОРА НА ОСНОВЕ ЛИПОСОМАЛЬНОЙ ФОРМЫ ТЕТРА-3-ФЕНИЛТИОФТАЛОЦИАНИНА ГИДРОКСИАЛЮМИНИЯ У МЫШЕЙ

А.П. Будько[1], З.Г. Дейчман[1], Г.А. Меерович[2,3], Л.М. Борисова[1], И.Г. Меерович[4], А.В. Ланцова[1], Н.Ю. Кульбачевская[1]

[1]ФГБУ «НМИЦ онкологии им. Н.Н. Блохина» Минздрава России, Москва, Россия
[2]Институт общей физики им. А.М. Прохорова Российской академии наук, Москва, Россия
[3]Национальный исследовательский ядерный университет МИФИ, Москва, Россия
[4]Институт биохимии им. А.Н. Баха, Федеральный исследовательский центр «Фундаментальные основы биотехнологии» Российской академии наук, Москва, Россия

Резюме

Настоящая работа посвящена исследованию фармакокинетики фотосенсибилизатора инфракрасного диапазона на основе тетра-3-фенилтиофталоцианина гидроксиалюминия в стабилизированной липосомальной лекарственной форме. Исследования проводили на половозрелых мышах-самках. Фотосенсибилизатор вводили мышам однократно внутривенно в дозе 6 мг/кг. Оценку динамики накопления фотосенсибилизатора в тканях и органах мышей проводили в интервалах времени от 5 мин до 7 сут с использованием спектрально-флуоресцентного метода. Максимальное накопление фотоактивной формы фотосенсибилизатора было зарегистрировано в легких (32 мкг/г в интервале 5–30 мин после введения), печени (20,8 мкг/г в интервале 4–24 ч после введения) и селезенке (28 мкг/г через 4 ч после введения). При этом в печени и селезенке к концу срока наблюдения (7 сут после введения) продолжали определяться следовые количества фотоактивной формы фотосенсибилизатора – расчетная концентрация составляла 0,5–1 мкг/г. Хуже всего фотосенсибилизатор накапливался в мышцах и коже. При этом в коже флуоресценция фотосенсибилизатора определялась практически сразу, и концентрация его оставалась на одном уровне (1,2–1,5 мкг/г) до 3 сут наблюдения. В мышцах концентрация фотосенсибилизатора достигала значения 1,5 мкг/г через 15 мин после введения, после чего постепенно снижалась и к 24 ч составила 0,25 мкг/г. Через 7 сут после введения, значения концентрации фотосенсибилизатора в коже и мышцах находились ниже предела детектирования. Исследования подтвердили, что ПЭГилирование липосомальной лекарственной формы фотосенсибилизатора замедляет процесс его захвата ретикуло-эндотелиальной системой. Показано, что фотосенсибилизатор длительно циркулирует в крови и органах мышей, распределение заканчивается только к 4 ч после введения.

Ключевые слова: фотосенсибилизатор, фармакокинетика, флуоресценция.

Для цитирования: Будько А.П., Дейчман З.Г., Меерович Г.А., Борисова Л.М., Меерович И.Г., Ланцова А.В., Кульбачевская Н.Ю. Изучение фармакокинетики фотосенсибилизатора на основе липосомальной формы тетра-3-фенилтиофталоцианина гидроксиалюминия у мышей // Biomedical photonics. – 2018. – Т. 7, № 4. – С. 16–22. doi: 10.24931/2413–9432–2018–7–4–16–22.

Контакты: Будько А.П., e-mail: apbudko@mail.ru

Introduction

Photodynamic therapy (PDT) is widely used for the treatment of malignant tumors, especially in cases of their surface and intracavitary location. The desired effect on the deep layers of large tumors is achieved with the use of photosensitizers (PS) of near infrared (IR) range [1]. The use of liposomal dosage forms (LLF) makes it possible to use new effective hydrophobic and hydrophilic substances in PDT, to increase the selectivity of PS accumulation in the tumor compared to the surrounding tissues and the effectiveness of the technique as a whole [1, 2].

For preclinical studies of the developed dosage form, including that on the basis of PS, it is necessary to study the pharmacokinetics [1–3]. This study is to determine the concentration of the active substance in various organs, tissues and body fluids at certain times after the administration and provides information on the duration of circulation of the PS in the body, target organs, which makes it possible to correlate the concentration and dosage of the PS with the pharmacological effect [4].

One of the most important requirements for pharmacokinetic studies is a wide dynamic range of the measurement method and tools, which must be at least three orders of magnitude.

Chromatographic, spectrophotometric, flame emission [5], atomic absorption [6], optical-spectral and spectral-fluorescent [7–11], and a number of other methods are used to determine the concentration of drugs in biological media. However, in the study of pharmacokinetics of PS, serious issues arise in connection with the use of many conventional methods of quantitative determination of the substance. Thus, when performing chromatography and spectrophotometry, it is necessary to extract the studied substance as fully as possible from the organs and tissues, including skin (it is the accumulation of PS in the skin that leads to negative side effects), which is quite difficult, especially in the case of quantitative determination of tetrapyrroles, to which the majority of PS belong. The task is even more complicated in the case when nanostructured PS based on hydrophobic substances is used (including the PS studied), since at different time after the introduction, some of the active substance molecules remain in the nanocarriers, whereas the other part is already transferred to the cell structure.

Flame emission and atomic absorption methods of elemental analysis [5,6], which can be used for the analysis without extraction of the studied pharmaceutical substances from tissues, have a limited dynamic range, especially for substances that consist of the same chemical elements as the body tissues (H, N, C, O) and do not contain rare elements, for example, metal atoms. The atomic absorption method was used by P. H. Brun et al. to study the pharmacokinetics of the Tookad photosensitizer in the blood and major internal organs, and the dynamics of its content in organs and tissues was evaluated by the intensity of the line of palladium included in Tookad [6].

At present, optical-spectral and spectral-fluorescent methods are used to determine the concentration of active substances in biological samples, in particular PS with characteristic absorption and fluorescence bands [7–11]. The use of equipment with high spectral resolution provides high sensitivity of such methods [10].

The purpose of this study was to investigate PS pharmacokinetics on the basis of tetra-3-phenylthiophthalocyanine hydroxylamine (3-$(PhS)_4$-PcAlOH) in LLF when administered intravenously to mice at a dose of 6 mg/kg.

Materials and methods

The studies of pharmacokinetics of PS were conducted on the basis of the substance developed in FSBI «N. N. Blokhin Russian Cancer Research Centre» of the Ministry of Healthcare of the Russian Federation LLF hydrophobic photoactive substance of tetra-3-phenylthiophthalocyanine hydroxyaluminium (abbr. 3-$(PhS)_4$-PcAlOH) (Fig. 1), created in FSUE «SRC «NIOPIK». The spectral absorption maximum of 3-$(PhS)_4$-PcAlOH corresponds to a wavelength of 717 nm. Stabilized LLF liposomes included 3-$(PhS)_4$-PcAlOH, lecithin lipids (USP30-NF25, P. 1145, Lipid GmbH, Germany) and cholesterol (USP30-NF25, P. 1101, Avanti Polar Lipids, Inc., USA), sucrose (FS.2.1.0034.15 GOST 5833–75, KHIMMED, Russia) as a cryoprotector, PEG-2000-DSPE ((1,2-dystearoyl-*sn*-glycero-3-phosphoethanolamine-[methoxy-(polyethylene-glycol)-2000] ammonium salt), Avanti Polar Lipids, Inc., USA). for the reduction of liposome capture by the reticuloendothelial system and a longer period of their circulation in blood [12–16].

Studies were carried out on 50 sexually mature female mice hybrids (C57Bl/6_J×DBA/2) F1, weighing 20–22 g, bred at FSBI «N. N. Blokhin Russian Cancer Research Centre» of the Ministry of Healthcare of the Russian Federation. The animals were randomly arranged into 10 groups of 5 animals in each.

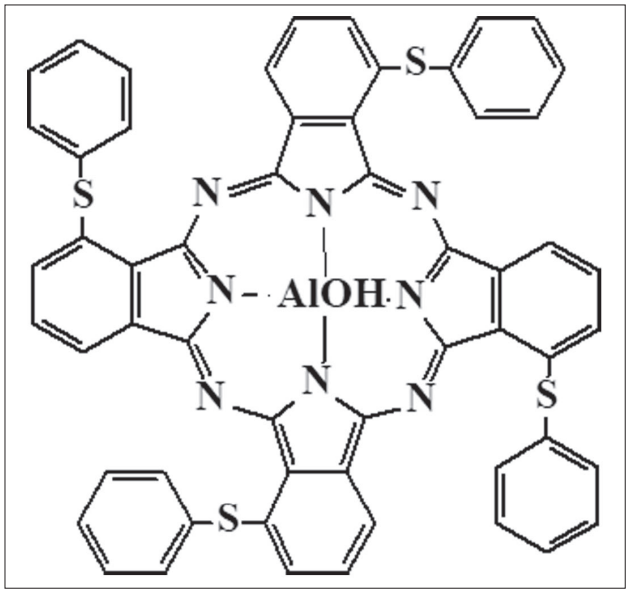

Рис. 1. Химическая формула тетра-3-фенилтиофталоцианина гидроксиалюминия
Fig. 1. Chemical formula of hydroxyaluminium tetra-3-phenylthiophthalocyanine

All animals were healthy and had a veterinary certificate of quality and of the health status. The animals were kept at an air temperature of 20–23 °C and relative humidity of 60–65% in the conditions of natural light and forced ventilation, on a litter of wood chips sterilized in a dry-air sterilizer. Animals were given standard industrial certified briquetted, fixed shelf life, feed for rodents. Feeding was done at the same time. Animals had free access to food and water.

All the experiments were performed in accordance with the recommendations of Good Clinical Practice [17].

Lyophilisate LLF 3-$(PhS)_4$-PcAlOH was redispersed with injection-grade water, 5.8 ml per vial, so that the content of 3-$(PhS)_4$-PcAlOH in the dispersion was 0.25 mg/ml. The volume of the dispersion for the injection was calculated based on the data on the body weight of the animal, and the dispersion was injected once by stream infusion into the tail vein, at a dose of 6 mg/kg.

The equipment and materials included a mechanical homogenizer (GlasCol, USA), Heildolph Reax Top vortex (Heidolph, Germany), Microman 1000 positive-displacement pipettes (Gilson, France), 24-hole plates with 16-millimeter holes 3424 MACG II for tissue culture (Costar, USA), distilled water.

The study of fluorescence was performed with the use of a modified laser electronic spectrum analyzer to LESA-01-«Biospec» (OOO «BIOSPEC», Russia). The dynamic range of the fluorescence signals recorded by the spectroanalyzer was extended to 3.5 orders of magnitude thanks to an additional algorithm for automatic control of the photosensor accumulation time. The linearity of response of the spectroanalyzer was established on samples of liposomal dispersions of 3-$(PhS)_4$-PcAlOH in distilled water with concentrations of 0.01 mg/ml 0.05 mg/ml; 0.1 mg/ml; 0.5 mg/ml; 2 mg/ml; 10 mg/ml; 25 mg/ml; 50 mg/ml and 0 (water as the control sample).

The statistical analysis was performed with the use of regular tools of Excel 2003 for Windows.

The preparation for the study of pharmacokinetics was performed as follows. The animals were killed by decapitation after 5 min, 15 min, 30 min, 1 h, 2 h, 4 h, 24 h, 48 h, 72 h and 168 h after the administration of the PS, after which blood was extracted from the jugular vein and heparin was added as an anticoagulant.

Samples of tissues and internal organs of mice (liver, kidneys, lungs, spleen, heart, muscle and skin) were obtained surgically. Liver, kidneys, and muscles were separated, reduced to a small size with eye scissors in a Petri dish on ice and divided into samples weighing 300g±1 mg, to which 1.5 ml of distilled water was added, followed by homogenization in glass on a mechanical homogenizer. For the spleen, lungs, heart and skin (skin samples were separated from subcutaneous tissue by scraping), the sample

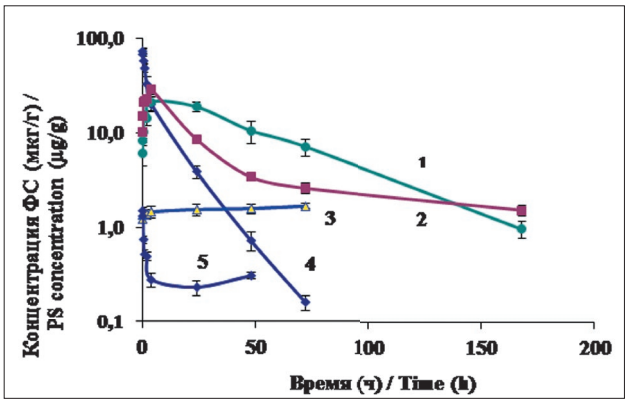

Рис. 2. Зависимость концентрации 3-(PhS)$_4$-PcAlOH от времени после его внутривенного введения в дозе 6 мг/кг в разных органах и тканях мышей: 1 – печень; 2 – селезенка; 3 – кожа; 4 – кровь; 5 – мышцы
Fig. 2. The dependence of 3-(PhS)$_4$-PcAlOH concentration on time after its intravenous administration at a dose of 6 mg/kg in different organs and tissues of mice: 1 – liver; 2 – spleen; 3 – skin; 4 – blood; 5 – muscle

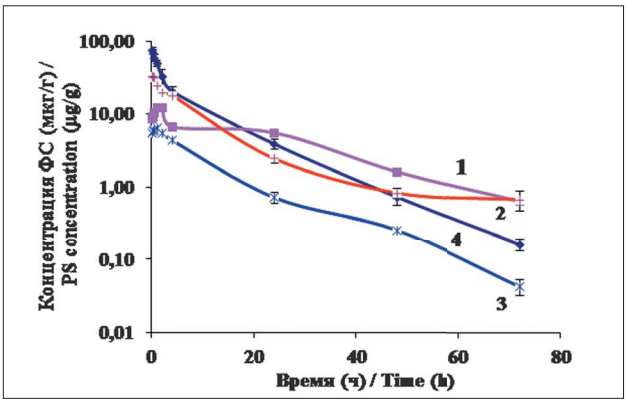

Рис. 3. Зависимость концентрации 3-(PhS)$_4$-PcAlOH от времени после его внутривенного введения в дозе 6 мг/кг в разных органах и тканях мышей: 1 – почки; 2 – легкие; 3 – сердце; 4 – кровь
Fig. 3. The dependence of 3-(PhS)$_4$-PcAlOH concentration on time after its intravenous administration at a dose of 6 mg/kg in different organs and tissues of mice: 1 – kidneys; 2 – lungs; 3 – heart; 4 – blood

weight was 100g±1 mg, the amount of water added decreased proportionally. The amount of homogenate equivalent to 100 mg of tissue was pipetted and transferred to the wells of the plates for subsequent measurement of fluorescence. Water was added in proportion to 100 mcl of blood.

Fluorescence of 3-(PhS)$_4$-PcAlOH in homogenates of samples was excited by laser radiation with a wavelength of 633 nm and recorded in the spectral range of 720–770 nm, and its concentration was determined by the integral intensity of fluorescence normalized by the intensity of the exciting laser radiation signal. To convert the values of fluorescence intensity into the values of PS concentration in the tissue, calibration curves were constructed by adding a known amount of PS to biological samples. Experimental and calibration samples underwent the same treatment.

Calibration showed that the dependence of the normalized integral fluorescence intensity on the concentration of 3-(PhS)$_4$-PcAlOH in samples within a wide range (for blood, within 0.1 to 129 μg/ml) is linearly dependant on the concentration, and with an accuracy of 6% for all organs it can be described by the function

$$I = k \times C,$$

where k = 27.99 $(\mu g/g)^{-1}$ for the measurement conditions recorded in the study, I is the normalized integral fluorescence intensity, and C is the concentration.

The ratio obtained from the calibration was used to quantify the concentration of 3-(PhS)$_4$-PcAlOH in the organs and tissues under examination.

Results and discussion

The dependences of the concentration of 3-(PhS)$_4$-PcAlOH in the blood and major organs and tissues (liver, spleen, kidneys, muscle, skin, heart, lungs) on the duration of the time interval between the introduction of the PS and the measurement of fluorescence in organs and tissues are shown in Fig. 2, 3.

The values of PS concentrations presented in the figures are the arithmetic mean of the obtained data and are accompanied by a confidence interval (p=95% at n=5).

The concentration in the blood 5 minutes after administration is 73.4 μg/l, going down to 3.9 μg/l over 24 h.

In the lungs, the maximum concentration of 32 μg/g is reached after 5 min of observation, does not change for 30 min, and then slowly decreases: the concentration drops to 2.45 μg/g over 24 hours. In the lungs, heart and kidneys there is no phase of growth of concentration 3-(PhS)$_4$-PcAlOH at the beginning of observation.

In the liver, the concentration of 3-(PhS)$_4$-PcAlOH increases from 6.2 μg/g after 5 min of observation to 20.8 μg/g after 4 h, remains at this level for up to 24 h and then slowly decreases to 0.5 μg/g for 168 h.

In the spleen, the concentration increases from 8.2 μg/g after 5 min of observation to 28 μg/g after 4 hours, then rapidly decreases to 8.5 μg/g to 24 hours, but is observed for up to 168 h.

In muscles, the concentration of 3-(PhS)$_4$-PcAlOH is maximal by 15 min after administration and is 1.5 μg/g, after which it decreases to 24 h to 0.25 μg/g.

In the kidneys, the maximum concentration of 12.5 μg/g is achieved by 2 h of observation, then by 4 h it is reduced 2 times to 6.64 μg/g, and by 72 h, to 0.65 μg/g.

In the skin (homogenized, without subcutaneous tissue), the concentration of 3-(PhS)$_4$-PcAlOH gradually increases from 1.2 μg/g after 4 h to 1.7 μg/g after 72 h after administration.

Таблица 1
Фармакокинетические параметры
Table 1
Pharmacokinetic parameters

Орган, ткань Organ, tissue	Параметры Parameters						
	C_0 мкг/мл μg/ml	V_1 мл ml	V_b мл ml	AUC мкг×ч/мл μg×h/ml	Cl_{tot} мл/ч ml/h	$T_{0,5a}$ час h	$T_{0,5b}$ час h
Кровь Blood	76,9	1,73	4,32	411,43	0,32	0,96	9,76

By 168 h of observation, the concentration values of 3-$(PhS)_4$-PcAlOH in the skin, kidneys, lungs, heart, and muscles are below the detection limit.

The obtained results allowed to calculate the following pharmacokinetic parameters in accordance with [18] for the dependence of PS concentration/time in the blood of mice after intravenous administration of 3-$(PhS)_4$-PcAlOH at a dose of 6 mg/kg: C_0 is the calculated concentration in the blood at the time of observation: 0 h; V_1 is the apparent estimated volume of dose distribution at the time of observation0 h;

V_b : kinetic volume of distribution;

AUC – area under the curve of «concentration – time»;

Cl_{tot}: total clearance, i. e. the volume of blood cleared from the pharmaceutical product over the time unit;

$T_{0.5a}$ is the distribution half-life of the pharmaceutical agent, the fast phase of the concentration decline;

$T_{0.5b}$ is the elimination half-life of the drug, the slow phase of the concentration decline.

It follows from the obtained data that the concentration-time dependence for blood is described by the two-component model equation. The distribution phase, with its rapid decrease in the concentration of 3-$(PhS)_4$-PcAlOH in the blood, is characterized by a high value of $t_{0.5a}$=0.96 h. The analysis of the data (first of all, of the high value of $T_{0.5a}$) points in the long circulation of LLF 3-$(PhS)_4$-PcAlOH in the blood, the distribution ends up to 4 hours after its introduction. High concentrations of 3-$(PhS)_4$-PcAlOH in the organs of the reticuloendothelial system (liver, spleen) are achieved only 4 h after administration. These data are consistent with the findings [14–16] that PEGylation reduces the capture of liposomes by the organs of the reticuloendothelial system, and extravasation of liposomes through the defects of the endothelial layer of neovascularization due to prolonged circulation leads to an increase in the level and selectivity of PS accumulation in the tumor. This correlates with the results obtained in the study of the level and selectivity of accumulation of the studied PS on tumor models [11], where the highest values of the level and selectivity of accumulation were observed 4–7 hours after its introduction (depending on the selected tumor model), and this time interval was recognized as the appropriate timeframe for the start of irradiation as a part of PDT.

The excretion phase with the slow decrease in the concentration of PS in the blood continues to 72 hours after administration: $T_{0.5b}$= 9.76 h.

Based on the value of V_1, the apparent volume distribution at the initial time for LLF, PS is distributed only in the blood. The value of the kinetic volume of V_b distribution is about 21% of the body volume of the animal.

The highest values of the area under the AUC curve were obtained in the liver and the spleen (2.3 and 1.6 times, respectively, higher than in the blood); in the kidneys, the ratio of AUC_{tissue}/AUC_{blood} was 0.7. The organs of FS accumulation are the spleen, the liver and the lungs.

Таблица 2
Площадь под кривой зависимости концентрация-время AUC для тканей мышей, соотношение площадей $AUC_{ткани}/AUC_{кровь}$
Table 2
Area under curve AUC for tissue, area ratio AUC_{tissue}/AUC_{blood}

Орган, ткань Organ, tissue	AUC мкг×ч/мл AUC μg×h/ml	$AUC_{ткани}/AUC_{крови}$ AUC_{tissue}/AUC_{blood}
Печень Liver	959,7	2,3
Почки Kidneys	275,4	0,7
Легкие Lungs	342,8	0,8
Селезенка Spleen	669,4	1,6
Мышцы Muscles	22,1	0,1
Сердце Heart	87,7	0,2
Кожа Skin	111	0,3

The kidneys and probably the liver are the organs responsible for PS excretion.

Conclusion

A method was developed for the preparation of biological samples for quantitative determination of concentration of PS.

The study examined the pharmacokinetics of the photosensitizer based on tetra-3-phenylthiophthalocyanine hydroxyaluminium in liposomal dosage form.

High (more than 20 μg/g) concentration values are observed in the liver, spleen, and, in the first hour of observation, in the lungs. After 24 hours of observation, the values of PS concentration are high enough in all organs. Traces of PS are detected in the liver and spleen in 168 h.

It was confirmed that the PEGilation of the liposomal drug form of PS slows down the process of its capture by the reticuloendothelial system. PS long circulates in the blood and organs of mice, with the distribution ending only 4 hours after administration.

The study was carried out with the financial support of the Russian Federal Property Fund (No. 17–07–01568) .

REFERENCES

1. Meerovich I.G., Sanarova E.V., Meerovich G.A., Volkov K.A., Negrimovsky V.M., Derkacheva V.M., Barkanova S.V., Lukyanets E.A., Oborotova N.A., Smirnova Z.S., Borisova L.M., Lantsova A.V., Polozkova A.P., Orlova O.L., Loschenov V.B., Umnova L.V., Baryshnikov A.Yu., Vorozhtsov G.N. Near-infrared photosensitizers based on nanostructured forms of phthalocyanine derivatives, *Russian Journal of General Chemistry*, 2015, vol. 85(1), pp. 280–288. doi: 10.1134/S1070363215010430
2. Baryshnikov A.Ju. Borisova L.M., Vorozhtsov G.N., Gerasimova G.K., Davydov M.I., Derkacheva V.M., Kokareva V.I., Kubasova I.Ju., Loshchenov V.B., Luzhkov Ju.M., Lukyanets E.A., Meerovich G.A., Meerovich I.G., Oborotova N.A., Polozkova A.P. Smirnova Z.S. Stratonnikov A.A. *Fotosensibilizator, liposomalnaya forma fotosensibilizatora i sposob provedeniya fotodinamicheskoi terapii* [Photosensitizing agent, liposomal formulation of photosensitizing agent and method for carrying out photodynamic therapy]. Patent RF no. 2257898, 2005.
3. Sanarova E., Meerovich I., Lantsova A., Kotova E., Shprakh Z., Polozkova A., Orlova O., Meerovich G., Borisova L., Lukyanets E., Smirnova Z., Oborotova N., Baryshnikov A. Thiosens liposomal dosage form technology development and photodynamic efficiency assessment, *J. Drug Delivery Science& Technology*, 2014, Vol. 24(4), pp.315–319.
4. *Rukovodstvo po provedeniyu doklinicheskih issledovanii lekarstvennyh sredstv. Chast' pervaya* [A guide to preclinical drug research. Part 1], ed. A.N. Mironov. Moscow: Grif&K Publ., 2012. 944 p.
5. Garifzyanov A.R. *Emissionnaya fotometriya plameni i atomno-absorbcionnaya spektroskopiya: elektronnoe uchebnoe posobie* [Emission photometry of flame and atomic absorption spectroscopy: an electronic textbook for 2nd year students]. Kazan', Kazan' state university Publ. 94 p.
6. Brun P.H., DeGroot J.L., Dickson E.F., Farahani M., Pottier R.H. Determination of the in vivo pharmacokinetics of palladium-bacteriopheophorbide (WST09) in EMT6 tumour-bearing Balb/c mice using graphite furnace atomic absorption spectroscopy, *Photochem Photobiol Sci.*, 2004, vol. 3(11–12), pp. 1006–1010.
7. Kalenkov G.S., Kalenkov S.G., Shtan'ko A.E. Hyperspectral holographic Fourier-microscopy, *Kvantovaya elektronika*, vol. 45, no 4, pp. 333–338.
8. Stratonnikov A.A., Meerovich G.A., Ryabova A.V., Savelieva T.A., Loschenov V.B. Application of backward diffuse reflection spectroscopy for monitoring the state of tissues in photodynamic therapy, *Kvantovaya elektronika*, 2006, vol. 36(12), pp. 1103–1110. (in Russian)
9. Loschenov V.B., Lin'kov K.G., Savelieva T.A., Loschenov M.V., Model S.S., Borodkin A.V. Hardware and tool equipment for fluorescence

ЛИТЕРАТУРА

1. Meerovich I.G., Sanarova E.V., Meerovich G.A. et al. Near-infrared photosensitizers based on nanostructured forms of phthalocyanine derivatives // Russian Journal of General Chemistry. – 2015. – Vol. 85(1). – P.280–288. doi: 10.1134/S1070363215010430
2. Барышников А.Ю., Борисова Л.М., Ворожцов Г.Н. и др. Фотосенсибилизатор, липосомальная форма фотосенсибилизатора и способ проведения фотодинамической терапии // Патент РФ № 2257898. – 2005.
3. Sanarova E., Meerovich I., Lantsova A., et al. Thiosens liposomal dosage form technology development and photodynamic efficiency assessment // J. Drug Delivery Science& Technology – 2014. – Vol. 24(4). – P.315–319.
4. Руководство по проведению доклинических исследований лекарственных средств. Часть первая // под ред. А.Н. Миронова. –М.: Гриф и К., 2012. – 944 с.
5. Гарифзянов А.Р. Эмиссионная фотометрия пламени и атомно-абсорбционная спектроскопия: электронное учебное пособие. – Казань: Казанский государственный университет, 2009. – 94 с.
6. Brun P.H., DeGroot J.L., Dickson E.F., et al. Determination of the in vivo pharmacokinetics of palladium-bacteriopheophorbide (WST09) in EMT6 tumour-bearing Balb/c mice using graphite furnace atomic absorption spectroscopy // Photochem Photobiol Sci. – 2004. – Vol. 3(11–12) . – P. 1006–1010.
7. Каленков Г.С., Каленков С.Г., Штанько А.Е. Гиперспектральная голографическая фурье-микроскопия // Квантовая электроника. – 2015. – Т. 45(4) . – С.333–338.
8. Стратонников А.А., Меерович Г.А., Рябова А.В. и др. Использование спектроскопии обратного диффузного отражения света для мониторинга состояния тканей при фотодинамической терапии // Квантовая электроника. – 2006. – Т. 36(12). – С. 1103–1110.
9. Лощенов В.Б., Линьков К.Г., Савельева Т.А. и др. Аппаратурное и инструментальное обеспечение флюоресцентной диагностики и фотодинамической терапии // Фотодинамическая терапия и фотодиагностика. – 2013. –Т. 2, № 3. – С. 17–25.
10. Reshetnikov A.V., Ponomarev G.V., Ivanov A.V., et al. Novel drug form of chlorin e6 // Proc. SPIE – 2000. – Vol. 3909. – P. 124–129.
11. Меерович Г.А., Борисова Л.М., Будько А.П. и др. Исследование уровня и селективности накопления липосомальной формы фотосенсибилизатора тетра-3-фенилтиофталоцианина гидроксиалюминия на опухолевых моделях мышей при разных способах перевивки // Российский биотерапевтический журнал. – 2017. – Т. 16, № 4 .– С. 74–79.
12. Abra R.M., Bankert R.B., Chen F., et al. The next generation of liposome delivery systems: recent experience with tumor-targeted,

diagnostics and photodynamic therapy, *Fotodinamicheskaya terapiia I fotodiagnostika*, 2013, vol. 2, no 3, pp. 17–25. (in Russian).
10. Reshetnikov A.V., Ponomarev G.V., Ivanov A.V., Abakumova O.Yu., Tsvetkova T.A., Karmenyan A.V., Rebeko A.G., Baum R.Ph. Novel drug form of chlorin e6, *Proc. SPIE*, 2000, vol. 3909, pp. 124–129.
11. Meerovich G.A., Borisova L.M., Bud'ko A.P., Kiseleva M.P., Nikolaeva L.L., Meerovich I.G., Lantsova A.V., Chernova S.V., Oborotova N.A. Study of the level and selectivity of accumulation of the liposomal form of the hydroxyaluminum tetra-3-phenylthiophthalocyanine photosensitizer on tumor models of mice with different methods of inoculation, *Rossiiskii bioterapevticheskii jurnal*, 2017, vol.16, no 4, pp. 74–79. (in Russian).
12. Abra R.M., Bankert R.B., Chen F., Egilmez N.K., Huang K., Saville R., Slater J.L., Sugano M., Yokota S.J. The next generation of liposome delivery systems: recent experience with tumor-targeted, sterically-stabilized immunoliposomes and active-loading gradients, *J. Liposome Res.*, 2002, vol. 12, pp. 1–3.
13. Brown I. M., Giaccia A. I. The unique physiology of solid tumors: opportunities (and problems) for cancer therapy, *Cancer Res.*, 1998, vol. 58(7), pp. 1408–1416.
14. Allen T.M. Liposomes. Opportunities in drug delivery, *Drugs*, 1997, vol. 54(4), pp. 8–14.
15. Moghimi S.M., Hunter A.C., Murray J.C. Long-circulating and target-specific nanoparticles: theory to practice, *Pharmacol. Rev.*, 2003, vol. 53, pp. 283–318.
16. 16. Klibanov A.L., Maruyama K., Torchilin V.P., Huang L. Amphipatic polyethyleneglycols effectively prolong the circulation time of liposomes, *FEBS Lett*, 1990, vol. 268, pp. 235–238.
17. Bol'shakov O.P., Neznanov N.G., Babakhanyan H.V. Didactic and Ethical Aspects of Research on Biomodels and Experimental Animals, *Kachestvennaia klinicheskaia practika*, 2002, no 1, pp. 58–61. (in Russian).
18. Soloviov V.N., Firsov A.A., Filov V.A. *Farmacokinetica* [Pharmakokinetics]. Moscow, Medicine Publ., 1980. 223 p.

sterically-stabilized immunoliposomes and active-loading gradients // J Liposome Res. – 2002. – Vol. 12. – P. 1–3.
13. Brown I.M., Giaccia A.I. The unique physiology of solid tumors: opportunities (and problems) for cancer therapy // Cancer Res. – 1998. – Vol. 58(7) – P. 1408–1416.
14. Allen T.M. Liposomes. Opportunities in drug delivery // Drugs. – 1997. – Vol. 54(4). – P. 8–14.
15. Moghimi S.M., Hunter A.C., Murray J.C. Long-circulating and target-specific nanoparticles: theory to practice// Pharmacol. Rev. – 2003. – Vol. 53. – P. 283–318.
16. Klibanov A.L., Maruyama K., Torchilin V.P., Huang L. Amphipatic polyethyleneglycols effectively prolong the circulation time of liposomes // FEBS Lett. – 1990. – Vol. 268. – P. 235–238.
17. Большаков О.П., Незнанов Н.Г., Бабаханян Р.В. Дидактические и этические аспекты проведения исследований на биомоделях и на лабораторных животных // Качественная клиническая практика. – 2002. – № 1. – С.58–61.
18. Соловьев В.Н., Фирсов А.А., Филов В.А. Фармакокинетика. – Москва: Медицина, 1980. – 223 с.

CLUSTER ANALYSIS OF THE RESULTS OF INTRAOPERATIVE OPTICAL SPECTROSCOPIC DIAGNOSTICS IN BRAIN GLIOMA NEUROSURGERY

Osmakov I.A.[1], **Savelieva T.A.**[1,2], **Loschenov V.B.**[1,2], **Goryajnov S.A.**[3], **Potapov A.A.**[3]
[1]National Research Nuclear University MEPhI, Moscow, Russia
[2]Prokhorov General Physics Institute of the Russian Academy of Sciences, Moscow, Russia
[3]N.N. Burdenko National Scientific and Practical Center for Neurosurgery
of the Ministry of Healthcare of the Russian Federation, Moscow, Russia

Abstract

The paper presents the results of a comparative study of methods of cluster analysis of optical intraoperative spectroscopy data during surgery of glial tumors with varying degree of malignancy. The analysis was carried out both for individual patients and for the entire dataset. The data were obtained using combined optical spectroscopy technique, which allowed simultaneous registration of diffuse reflectance spectra of broadband radiation in the 500–600 nm spectral range (for the analysis of tissue blood supply and the degree of hemoglobin oxygenation), fluorescence spectra of 5-ALA induced protoporphyrin IX (Pp IX) (for analysis of the malignancy degree) and signal of diffusely reflected laser light used to excite Pp IX fluorescence (to take into account the scattering properties of tissues). To determine the threshold values of these parameters for the tumor, the infiltration zone and the normal white matter, we searched for the natural clusters in the available intraoperative optical spectroscopy data and compared them with the results of the pathomorphology. It was shown that, among the considered clustering methods, EM-algorithm and k-means methods are optimal for the considered data set and can be used to build a decision support system (DSS) for spectroscopic intraoperative navigation in neurosurgery. Results of clustering relevant to the pathological studies were also obtained using the methods of spectral and agglomerative clustering. These methods can be used to post-process combined spectroscopy data.

Keywords: optical spectroscopy, fluorescence, diffuse reflectance, 5-ALA, protoporphyrin IX, neurosurgery, gliomas, cluster analysis

For citations: Osmakov I.A., Savelieva T.A., Loschenov V.B., Goryajnov S.A., Potapov A.A. Cluster analysis of the results of intraoperative optical spectroscopic diagnostics in brain glioma neurosurgery, *Biomedical photonics,* 2018, vol. 7, no. 4, pp. 23–34. (in Russ.) 10.24931/2413–9432–2018–7–4–23–34.

Contacts: Osmakov I.A., e-mail: ilya.osmakov@gmail.com

КЛАСТЕРНЫЙ АНАЛИЗ РЕЗУЛЬТАТОВ ИНТРАОПЕРАЦИОННОЙ ОПТИЧЕСКОЙ СПЕКТРОСКОПИЧЕСКОЙ ДИАГНОСТИКИ В НЕЙРОХИРУРГИИ ГЛИАЛЬНЫХ ОПУХОЛЕЙ ГОЛОВНОГО МОЗГА

И.А. Осьмаков[1], **Т.А. Савельева**[1,2], **В.Б. Лощенов**[1,2], **С.А. Горяйнов**[3], **А.А. Потапов**[3]
[1]Национальный исследовательский ядерный университет «МИФИ», Москва, Россия
[2]Институт общей физики им. А.М. Прохорова Российской академии наук, Москва, Россия
[3]Национальный медицинский исследовательский центр нейрохирургии
имени академика Н. Н. Бурденко, Москва, Россия

Резюме

В работе представлены результаты сравнительного исследования методов кластерного анализа данных оптической интраоперационной спектроскопии при проведении операций по удалению глиальных опухолей различной степени злокачественности. Анализ проведен как для отдельных пациентов, так и для всей совокупности данных. Данные были получены методом комбинированной оптической спектроскопии, регистрирующим спектр диффузного отражения широкополосного излучения в диапазоне спектра 500–600 нм (с целью анализа кровенаполненности тканей и степени оксигенации гемоглобина), спектр флуоресценции индуцированного 5-аминолевулиновой кислотой протопорфирина IX (с целью анализа степени изменения тканей) и сигнал диффузно отраженного лазерного излучения, использовавшегося для возбуждения флуоресценции (с целью учета рассеивающих свойств тканей).

Для определения пороговых значений указанных параметров для опухоли, зоны инфильтрации и нормального белого вещества был проведен поиск естественных кластеров в имеющихся интраоперационных данных оптической спектроскопии и их сопоставление с результатами патоморфологической экспертизы. Было показано, что среди рассмотренных методов кластеризации EM-алгоритм и метод k-средних оптимальны для рассмотренного набора данных и могут быть использованы для построения системы поддержки принятия решений при спектроскопической интраоперационной навигации в нейрохирургии. Релевантные результатам патоморфологических исследований модели были также получены с помощью методов спектральной и агломеративной кластеризации. Эти методы могут быть использованы для постобработки данных комбинированной спектроскопии.

Ключевые слова: оптическая спектроскопия, флуоресценция, диффузное отражение, 5-АЛК, протопорфирин IX, нейрохирургия, глиомы, кластерный анализ.

Для цитирования: Осьмаков И.А., Савельева Т.А., Лощенов В.Б., Горяйнов С.А., Потапов А.А. Кластерный анализ результатов интраоперационной оптической спектроскопической диагностики в нейрохирургии глиальных опухолей головного мозга // Biomedical photonics. – 2018. – Т. 7, № 4 . – С. 23–34. doi: 10.24931/2413–9432–2018–7–4–23–34.

Контакты: Осьмаков И.А., e-mail: ilya.osmakov@gmail.com

Introduction

The incidence of cancer of the central nervous system is currently increasing steadily [1]. One of the main methods of their treatment is surgical removal of malignant tumors. However, the determination of the boundaries of glial tumors is a nontrivial task due to the peculiarities of their growth along the myelinated nerve fibers and vessels deep into the healthy white matter of the brain [2, 3], which leads to incomplete removal of the tumor and a high frequency of postoperative recurrences.

It is the infiltrating nature of the growth of glial tumors that necessitates the use of additional methods of their demarcation during surgery. At the same time, optical methods for determining the type and condition of biological tissues have a number of significant advantages: high speed, accuracy, non-invasive nature, a compact size of the working part of the tool. The most popular among optical methods is the registration of fluorescence markers of tumor changes of both endogenous and exogenous nature.

At the moment, the working tool based on the principle of optical detection of fluorescence used in neurosurgery is the Opmi Pentero microscope with Blue400 mode, which allows to observe the level of fluorescence (excited in the purple range of the spectrum) accumulation of protoporphyrin IX (PPIX) induced by 5-aminolevulinic acid (5-ALA) in tumor cells. The main disadvantage of this method is the subjectivity of the evaluation of the recorded signal by a neurosurgeon. It is the doctor who, largely at his/her own discretion, determines which brightness of fluorescence shall be considered to be a subthreshold level where tumor destruction must be stopped. And the tactics of surgeons in this regard may differ. Therefore, it is essential to use a quantitative approach to intraoperative analysis of the type of fabric which is supported by optical spectrum analysis. Moreover, in the case of a sufficiently large sample of morphologically verified conclusions, it is preferable to use not only numerical values but also the preliminary conclusions about the type of tissues.

In the case of one parameter characterizing the degree of tissue malignancy (fluorescence PPIX), determining the type of tissue only by the value of the parameter is a fairly trivial task. However, as the number of parameters increases, the task becomes more complex and the use of statistical methods of data analysis for a preliminary conclusion is required. Machine learning methods are ideally suited for solving this problem.

This work is devoted to the preliminary cluster analysis of spectroscopic data for individual patients, as well as for the entire data set, with the use of the built-in libraries in Python language. It describes an optical spectroscopy method that uses the analysis of fluorescence spectra of 5-ALA-induced PPIX and diffuse reflection spectra of tissues, with subsequent extraction of information from them on the absorbers in tissues and their light scattering properties. To determine the threshold values for the tumor, the infiltration zone and the normal level, it is necessary to search for natural clusters in the available intraoperative optical spectroscopy data and compare them with the results of pathomorphological examination.

Materials and methods

Intraoperative optical spectroscopy method

A device was developed for simultaneous registration of diffuse reflection spectra and laser-induced fluorescence, consisting of a spectroanalyzer (LASA-01-BIOSPEC), two radiation sources (helium-neon laser λ=632.8 nm and a halogen lamp), fiber-optic transfer system for the delivery of radiation to and from the tissue, as well as a personal computer with special software for registration and analysis of spectra in real time. The device uses a cross-filter system that allows the separation of the visible range of the spectrum into two areas: the registration of

the diffuse reflection spectrum and the fluorescence spectrum of PPIX.

During the measurements, the distal end of the fiber optic probe was brought closer to the tissue to the degree of contact without pressure. As a result of the measurement, the input of the spectrometer receives fluorescent, as well as broadband and laser radiation which is diffusely reflected by the tissue. The recorded spectral dependences are subjected to mathematical processing in accordance with the algorithms described in [4], in a real-time mode.

The scattering properties of the tissues were estimated by the intensity of the backward scattered laser radiation and are given in comparison with the doubled value of the unchanged cortex (since, according to the literature, the diffuse reflection signal from white matter in the visible range of the spectrum is on average twice higher than from gray matter). The fluorescence intensity was calculated as the ratio of PPIX fluorescence intensity in the range of 690–730 nm to the intensity of the backward scattered laser radiation. Fluorescent contrast was determined as the ratio of the fluorescence intensity of the tissue studied to the fluorescence intensity of the normal cortex. The examples of recorded spectra are shown in Fig. 1.

The calculation of the parameters for the analysis was made according to the following formulas:

$$FI_i = \frac{S_{[690..730],i}}{S_{[625..640],i}} \qquad FC_i = \frac{FI_i}{FI_{norm}}$$

$$ScC_i = \frac{S_{[625...640],i}}{k*S_{[625..640],norm}} \qquad Hb_{total,i} = [Hb]_i + [HbO_2]_i$$

$$HbC_i = \frac{Hb_{total,i}}{Hb_{total,norm}}$$

$$Sat(Hb)_i = \frac{HbO_{2i}}{Hb_{total,i}} \qquad Sat(Hb)C_i = \frac{Sat(Hb)_i}{Sat(Hb)_{norm}}$$

where *S* is the area under the graph in the range indicated in the lower index; *i* is the fluorescence intensity calculated from the current spectrum; *norm* is the fluorescence intensity calculated on the basis of the normal tissue spectrum (usually from the cortex at some distance from the tumor projection); *FI* is the fluorescence intensity; *FC* is the contrast of the tissue under study compared with the normal fluorescence intensity; *ScC* is the contrast of the tissue under study compared to the tissue which has normal light scattering level; *k* is the coefficient of the fluorescence intensity with due account for the differences in light scattering for white and gray matter (k=2 when used as the norm of gray matter, k=1 when used as the norm of white matter); *[Hb]* is the concentration of reduced hemoglobin; *[HbO_2]* is the concentration of oxygenated hemoglobin; Hb_{total} is the total concentration of hemoglobin in the tissue (blood filling); *Sat(Hb)* is the degree of hemoglobin oxygenation (oxygen saturation).

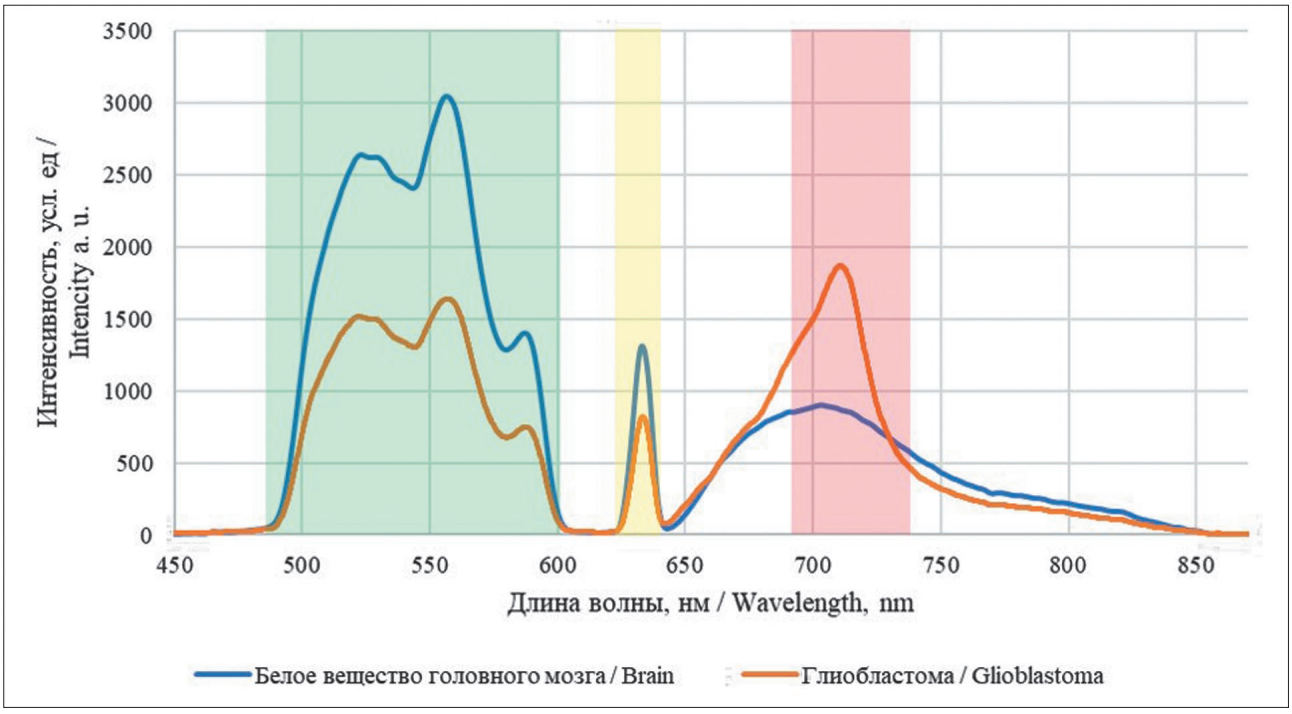

Рис. 1. Пример спектров различных типов тканей: зеленым цветом обозначена область оценки степени оксигенации, желтым – диффузного отражения лазерного излучения, красным – флуоресценции
Fig. 1. Example of spectra characteristic for different types of tissue: green – spectral range used for evaluation of oxygenation level, yellow – diffuse reflectance of laser light, red – fluorescence spectrum

Clinical data

The study retrospectively used the data from 13 patients. Three patients diagnosed with glioblastoma/astrocytoma from the sample underwent separate research. The training of the clustering algorithm was carried out on each patient separately, and then on the aggregate of the three, in order to compare the quality metrics on the test sample, which included the remaining patients. Thus, the algorithm was tested on the objects not included in the training sample. The patients were orally administered a solution of the hydrochloride of 5-aminolevulinic acid (Alasens product, manufacturer: FSUE «SRC «NIOPIK», Russia) calculated as 25 mg/kg body weight, 2–4 hours before tumor removal. Videofluoroscopy intraoperative navigation was performed with the use of operating microscope (Opmi Pentero, Carl Zeiss, Germany) with fluorescence module simultaneously with spectroscopic navigation device LESA-01-Biospec (OOO «BIOSPEC», Russia). 2 to 11 tissue samples were taken from each patient for subsequent histological analysis and comparison of its results with the data of spectroscopic examination. Each tissue sample corresponded to a number of spectra (from 1 to 10). Thus, 77 tissue samples and 876 spectra were analyzed, of which 335 were verified by histological conclusions. A scatter diagram of all verified objects is shown in Fig. 2.

Working with missing data

The specifics of the collected data is that the technical methods for simultaneous registration of all the parameters were not used in the early development and use of intraoperative optical spectroscopy method. It was only possible to measure the following pairs: the total concentration of hemoglobin in the tissues and the degree of its oxygenation or fluorescence intensity and the area under the peak of the echo signal. Due to this fact, some data was missing.

Missing data refers to empty parameter values of the objects. Their processing is a separate section of statistics and independent research work. In this study, the following standard methods of their processing were considered: removal, in which the sample was reduced 2 to 2.5 times, which is an impractical method; data zeroing led to the appearance of a set of objects with different histological labels at point 0; averaging by parameters, in which the algorithms obtained low quality metrics.

These unsatisfactory results led to the creation of a multi-step data processing strategy which included:

1. The division of data into complete and incomplete
2. The division of the complete data into the training sample and the test sample
3. The classification of incomplete data by diagnosis
4. The separation of data broken down by diagnoses in accordance with the types of tissues
5. Averaging by each type
6. The combination of training data and data averaged by type.

There were also patients who had only one pair of parameters. In such patients, the missing parameters were averaged by type with the parameters of all patients with the same diagnosis. Thus, the test sample included the objects with true parameters, and the training sample was made as large as possible. This strategy, in comparison with other methods of missing data processing, proved to have the highest quality metrics, the

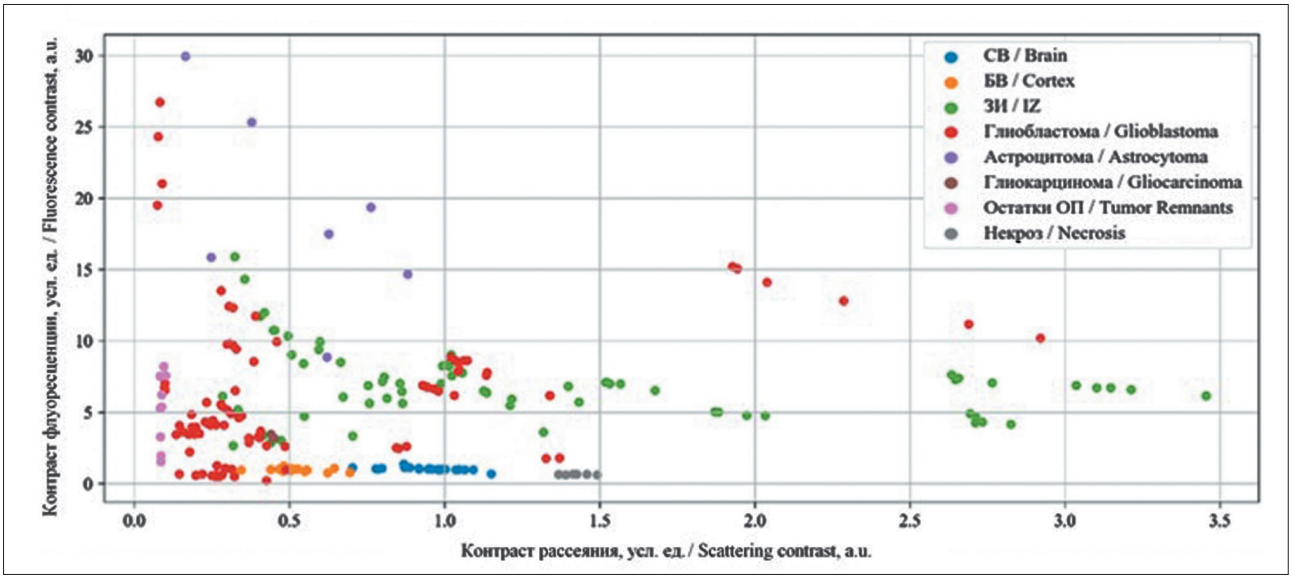

Рис. 2. Точечная диаграмма верифицированных данных, где СВ – серое вещество головного мозга, БВ – белое вещество головного мозга, ЗИ – зона инфильтрации, ОП – опухоль
Fig. 2. Scatter plot of verified data, where IZ – Infiltration Zone

largest number of successful algorithms, the preservation of most objects and the highest degree of interpretation.

Cluster analysis

For cluster analysis, the unsupervised learning approach was used. In this paper, we have considered the following methods of clustering: the k-means method, spectral clustering, expectation-maximization method (EM-algorithm), agglomerative clustering, and density clustering, the iterations of which are described below.

Before cluster analysis, the data underwent preliminary standardization, as it is necessary before such processing. This is to ensure that the weights selected in the algorithms are not operated with the parameters of different orders.

The k-means method. This is one of the most common methods used for primary data processing, which gained particular popularity after the publication of McQueen's study [5]. It involves choosing n-random clustering centers. Then, each object is compared to each center, and the object is assigned to the cluster to the center of which the object is the closest. Finally, the centers are calculated.

Spectral clustering method. In this method, similarity matrices are defined for the objects. Next, the two nearest objects are combined according to the similarity matrix so that the objects within the cluster are as different as possible from the objects of other clusters [6].

The EM-algorithm. The method is to maximize likelihood. It is based on the fact that the density of distribution probability for the objects in a sample is a weighted sum of the densities of probability in each cluster. All clusters are selected from a certain family of distributions, which are often families of normal distributions [7].

Agglomerative clustering method. In this method, pairwise distances between objects are sorted in ascending order, and each is assigned to its own cluster. Then a pair of the nearest clusters is selected and combined into one. (The search for the closest clusters can be performed with the use of various combination methods). After that, the number of centers is calculated.

Density clustering method. In this method, there must be a certain number of other points near the object within a certain radius; if this condition is not met, the object is labeled as noise.

From the specifics of the use of the clustering algorithms considered, it is possible to conclude that such methods as k-means and EM-algorithm can produce the output model of data clustering which can then be used to predict new objects.

The input parameters were chosen in the way that healthy objects were separated as much as possible from the rest of the sample into a separate cluster, but the number of clusters did not exceed 8. This is due to the fact that the number of histologically different objects may not exceed 8.

Quality metrics

In order to assess the quality of clustering results, various quality metrics are used. Such estimates must not depend on the label values themselves but only on the sample partition as such. In addition, true labels of objects are not always known, so it is necessary to have estimates that make it possible to evaluate the quality of clustering based on only an unlabeled sample.

There are external and internal quality metrics. The external metrics use the information about true clustering, while internal metrics use no external information and evaluate the quality of clustering only on the basis of the dataset. The optimal number of clusters is usually determined with the use of internal metrics.

Adjusted Rand Index (ARI). It is assumed that the true labels of the objects are known. This measure does not depend on the label values as such but only on the partitioning of the sample into clusters. Let n be the number of objects in the sample, then a is the number of pairs of objects that have the same labels and are in the same cluster, and b is the number of pairs of objects that have different labels and are in different clusters. The Rand Index then is:

$$RI = \frac{2(a+b)}{n(n-1)}$$

That is, it is the share of objects for which these partitions (initial and resulting from clustering) are «approved». Rand Index (*RI*) expresses the similarity of two different clusterings of the same sample. For this index to give values close to zero for random clustering with any n and any number of clusters, it is necessary to normalize it. This is how the Adjusted Rand Index is determined:

$$ARI = \frac{RI - E[RI]}{\max(RI) - E[RI]}$$

This measure is symmetric and does not depend on the values of the labels and their swapping. Thus, this index is a measure of the distance between various sample partitions. *ARI* takes values in the range [-1,1]. Negative values correspond to «independent» cluster partitions; values close to zero correspond to random partitions, and positive values indicate that two partitions are similar (coincide at $ARI = 1$).

Adjusted Mutual Information (AMI). This measure is very similar to *ARI*. It is also symmetric and does not depend on the values of the labels and their swapping. It is determined with the use of the entropy function, with the interpretation of sample splits as discrete distributions (the probability of the assignment to a cluster is equal to the share of objects in the cluster). The *AMI* index is defined as the mutual information for two distribu-

tions corresponding to the sample-to-cluster partitions. Intuitively, mutual information measures the proportion of information common to both partitions: how much the information on one of them reduces the uncertainty in respect of the other.

AMI index is determined in the way which is similar to the determination of *ARI*, making it possible to avoid the growth of the *AMI* index with the increase in the number of classes. It takes values in the range of [-1,1]. The values close to zero indicate the independence of the partitions, and those close to one, their similarity (coincidence at *ARI* = 1).

Homogeneity, completeness, V-measure. Formally, these measures are also defined with the use of entropy and conditional entropy functions, with the consideration of sample partitions as discrete distributions:

$$h = 1 - \frac{H(C|K)}{H(C)}$$

$$c = 1 - \frac{H(K|C)}{H(K)}$$

here *K* is the result of clustering, *C* is the true division of the sample into classes. Thus, *h* measures the degree to which each cluster consists of objects of the same class, and *c* measures the degree to which the objects of the same class belong to the same cluster. These measurements are not symmetrical. Both take on values in the range of [0,1], and larger values correspond to more accurate clustering. These measures are not normalized like *ARI* or *AMI* and, therefore, they depend on the number of clusters. Random clustering will not produce zero values in case of a large number of classes and a small number of objects. In these cases, it is preferable to use *ARI*. However, if the number of objects is more than 1000 and the number of clusters is less than 10, this problem is not so pronounced and can be ignored.

To account for both values, *h* and *c*, a *V*-measure is also introduced as their harmonic mean:

$$v = 2\frac{hc}{h + c}$$

It is symmetric and shows how much the two clusterings are similar to each other.

Silhouette. In contrast to the above metrics, this coefficient does not imply the knowledge of the true labels of objects and makes it possible to assess the quality of clustering with the use of only the (unlabeled) selection and the result of clustering. First, the silhouette is defined separately for each object. *a* is the average distance from this object to the objects from the same cluster, *b* is the average distance from this object to the objects from the nearest cluster (different from the one in which the object itself is). Then the silhouette of the object is the value:

$$s = \frac{b - a}{\max(a, b)}$$

The silhouette of a selection is the average value of the silhouette of the objects in that selection. Thus, a silhouette shows how the average distance to the objects of the same cluster differs from the average distance to the objects of other clusters. This value is in the range of [-1,1]. Values close to -1 correspond to the clustering variant with a high spread, values close to zero mean that clusters intersect and overlap, and values close to 1 correspond to «dense» clearly outlined clusters. Thus, the larger the silhouette, the more clearly the clusters are outlined, and they are compact, tightly grouped clouds of points.

With the silhouette, you can select the optimal number of clusters *k* (if it is not known in advance) and select the number of clusters that maximize the value of the silhouette. Unlike the previous metrics, the silhouette depends on the shape of the clusters, and reaches larger values on the more convex clusters obtained by algorithms based on the restoration of the distribution density.

To assess the quality of clustering, clusters were manually merged in such a way that healthy objects were in a separate cluster, and all other objects were combined into a cluster of pathology (not healthy ones). Thus, the obtained metrics will evaluate how well the used method distinguishes the healthy objects from the sick ones.

Results and discussion

Results of the analysis of data for individual patients

Patient G. Diagnosis: diffuse astrocytoma with pronounced polymorphism.

Patient G. had a sample of 12 objects. The quality metrics are presented in Table 1. The resulting models in the visualization can not be correlated with true representations. However, k-means and agglomerative clustering methods were able to group healthy tissues into a separate cluster, but the very model of data clustering turned out to have very broad boundaries, which allow fluorescence intensity above 7.5, which is not typical for a healthy brain area. Based on the results of the analysis of the data of this patient, it is obvious that these methods of processing should be used on sufficiently large samples.

For patient G., the methods that have the highest quality estimates are density clustering, k-means, and agglomerative clustering.

Patient S. Diagnosis: glioblastoma Grade IV.

As can be seen from Table 2, all algorithms except the density method showed equally good results in the

division of normal and pathologic samples into separate clusters. This is due to its features, which result in marking some objects as noise, greatly reducing its quality metrics. However, this method allocates objects that are close in time into separate clusters. This feature can be useful further on for the averaging of such objects in order to prevent them from making large weights in the measurements.

Patient S., in comparison with patient G., had a sample of 82 objects, that is, it was almost 6 times more numerous. Healthy tissues were well grouped into a separate cluster, as it can be seen by the example of the visualization of the agglomerative clustering results (Fig. 3*a*). The input parameters of clustering were selected in such a way that allows to differentiate healthy tissues from all others.

It is also worth noting that the obtained straight boundaries in the k-means method (Fig. 3*b*) are not relevant to the complex boundary between clusters found in the experiment, which is not apparent in the EM-algorithm (Fig. 3*c*). However, the EM algorithm did not have a gradient transition between clusters, which would be typical for infiltration zones and for the diffuse nature of glioblastomas. In addition, it is difficult to interpret the resulting model of data division into clusters, because healthy tissues were included in a large cluster with characteristics that differ from those for healthy tissues.

Patient B. Diagnosis: Glioblastoma**.**

Patient B. had a sample of 59 objects; the quality metrics of the obtained models are shown in Table 3. The best methods were EM-algorithm, spectral clusterization, k-means, agglomerative clustering. However, the values of these metrics are not high enough to use the resulting clustering models due to insufficient sample size.

Results of the analysis of the data set of all patients

To begin with, an analysis was carried out of the data set of those patients who were earlier considered separately.

Patients B. + G. + C.

The results of the processing of the integrated data of patients B., G. and S. are shown in Fig. 4 and in table 4. The high-quality metrics and the more predictable nature of the healthy tissue model make it possible to say that the increase of the sample has a positive impact on the comprehensive assessment of the results.

The clustering density method obtained an abnormally large number of clusters, more than 10. A more detailed study of this phenomenon showed that most clusters consist of objects which are close-standing in terms of the registration time, that is, very likely, these spectra corresponded to the same small area of tissue.

The quality assessment of B. + G. + C. models in other patients

Since the processing of the total data set of the three patients produced potentially plausible models, the data

Таблица 1
Метрики качества пациента Г. на отложенной выборке
Table 1
Quality metrics of held-out set for patient G.

Название Metric	AMI	ARI	Гомогенность Homogeneity	Полнота Completeness	V-мера V-measure	Силуэт Silhouette
ЕМ-алгоритм EM-algorithm	0,4666	0,6409	0,5183	0,6468	0,5754	0,2609
СК SC	0,4666	0,6409	0,5183	0,6468	0,5754	0,3502
ПК DC	9,8715	0,0000	9,8715	1,0000	1,9743	0,3705
k-средних k-means	1,0000	1,0000	1,0000	1,0000	1,0000	0.4551
АК AC	1,0000	1,0000	1,0000	1,0000	1,0000	0,4551

СК – спектральная кластеризация, ПК – плотностная кластеризация, АК – агломеративная кластеризация
SC – spectral clustering, DC – density-based clustering, AC – agglomerative clustering

were then used to evaluate the quality metrics on their basis, in respect of the data of patients for whom no clustering was performed.

Evaluation of the quality of predictions for patient D. (127 objects, 41 verified ones), patient L. (30 objects, 23 verified ones) and the remaining group of 9 patients (422 objects, 93 verified ones), on models obtained in patients B., G., S., is presented in table 5.

It can be seen from the obtained metrics that in all patients the EM-algorithm coped with the task almost perfectly, given that the test sample included some types of tissues that the algorithm had not dealt with before,

Таблица 2
Метрики качества пациента С. на отложенной выборке
Table 2
Quality metrics of held-out set for patient S.

Название Metric	AMI	ARI	Гомогенность Homogeneity	Полнота Completeness	V-мера V-measure	Силуэт Silhouette
ЕМ-алгоритм EM-algorithm	1,0000	1,0000	1,0000	1,0000	1,0000	0,2446
СК SC	1,0000	1,0000	1,0000	1,0000	1,0000	0,2446
ПК DC	0,4464	0,4411	1,0000	0,4548	0,6252	0,1153
k-средних k-means	1,0000	1,0000	1,0000	1,0000	1,0000	0,2446
АК AC	1,0000	1,0000	1,0000	1,0000	1,0000	0,2446

СК – спектральная кластеризация, ПК – плотностная кластеризация, АК – агломеративная кластеризация
SC – spectral clustering, DC – density-based clustering, AC – agglomerative clustering

Таблица 3
Метрики качества пациента Б. на отложенной выборке
Table 3
Quality metrics of held-out set for patient B.

Название Metric	AMI	ARI	Гомогенность Homogeneity	Полнота Completeness	V-мера V-measure	Силуэт Silhouette
ЕМ-алгоритм EM-algorithm	0,8133	0,9150	0,8710	0,8174	0,8434	0,4313
СК SC	0,8133	0,9150	0,8710	0,8174	0,8434	0,4313
ПК DC	0,3053	0,2838	0,7268	0,3192	0,4436	0,0815
k-средних k-means	0,8133	0,9150	0,8710	0,8174	0,8434	0,4313
АК AC	0,8133	0,9150	0,8710	0,8174	0,8434	0,4313

СК – спектральная кластеризация, ПК – плотностная кластеризация, АК – агломеративная кластеризация
SC – spectral clustering, DC – density-based clustering, AC – agglomerative clustering

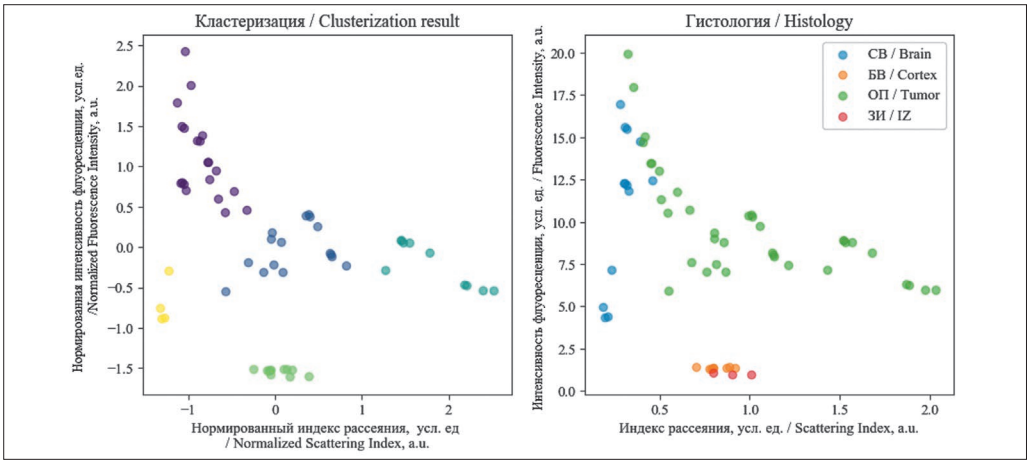

a

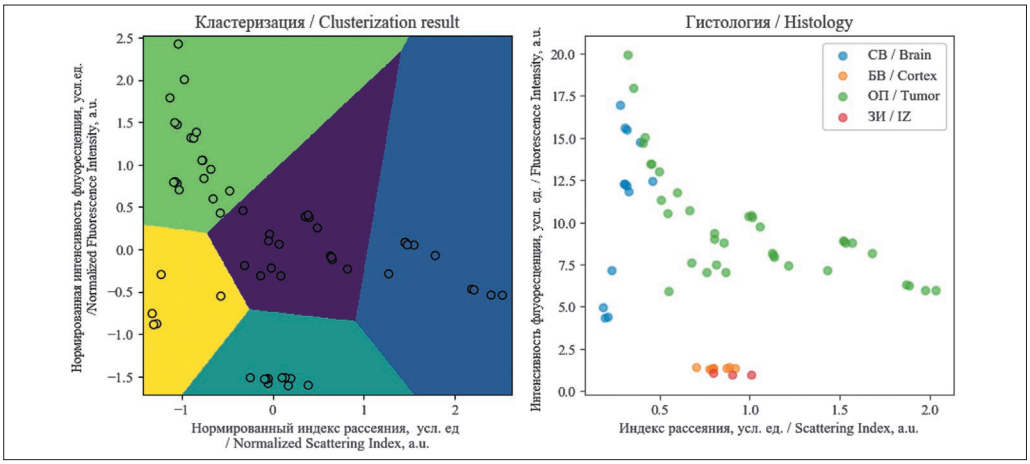

b

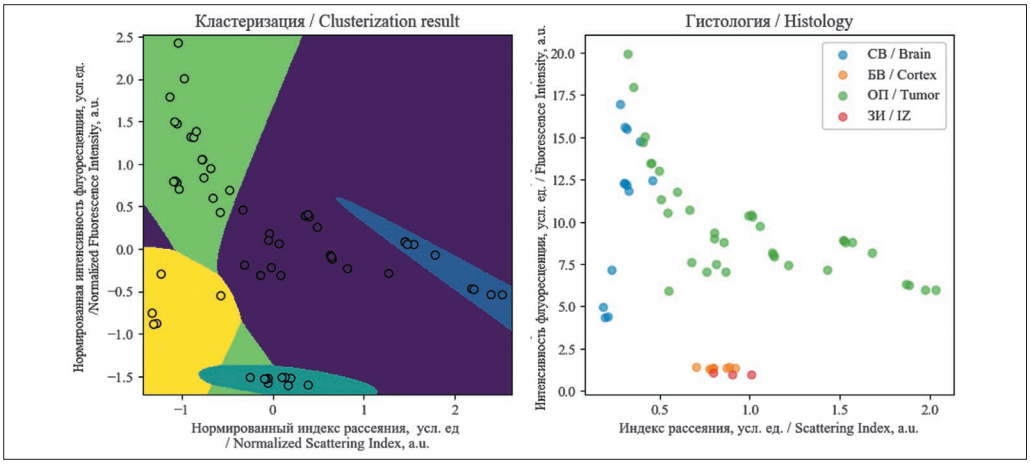

c

Рис. 3. Визуализация результатов пациента С. с применением различных методов кластеризации, в сравнении с реальным распределением объектов (справа), где СВ – серое вещество головного мозга, БВ – белое вещество головного мозга, ОП – опухоль, ЗИ – зона инфильтрации:

a – агломеративная кластеризация;
b – кластеризация k-средних;
c – кластеризация EM-алгоритмом

Fig. 3. Visualization of clusterization results (left) compared to actual distribution (right) for patient S., where IZ – infiltration zone:

a – aglomerative clusterization;
b – k-means clusterization;
c – EM-algorithm clusterization

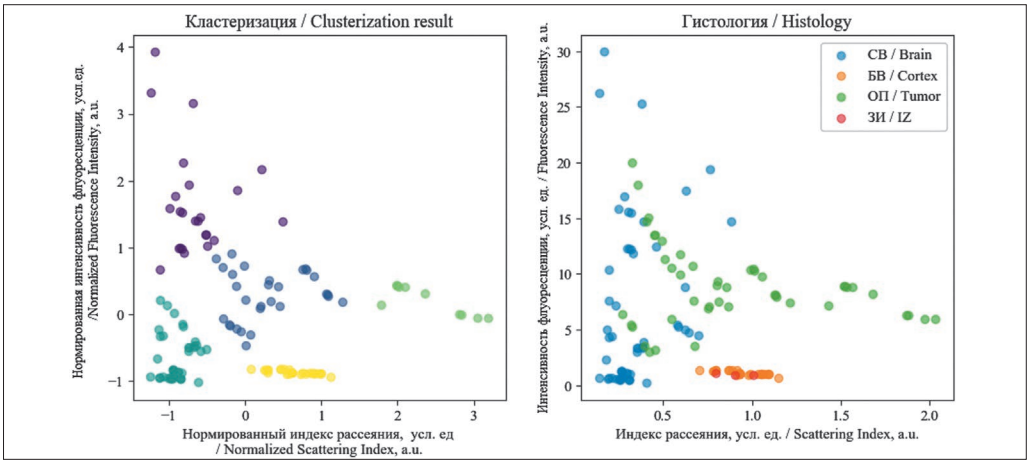

a

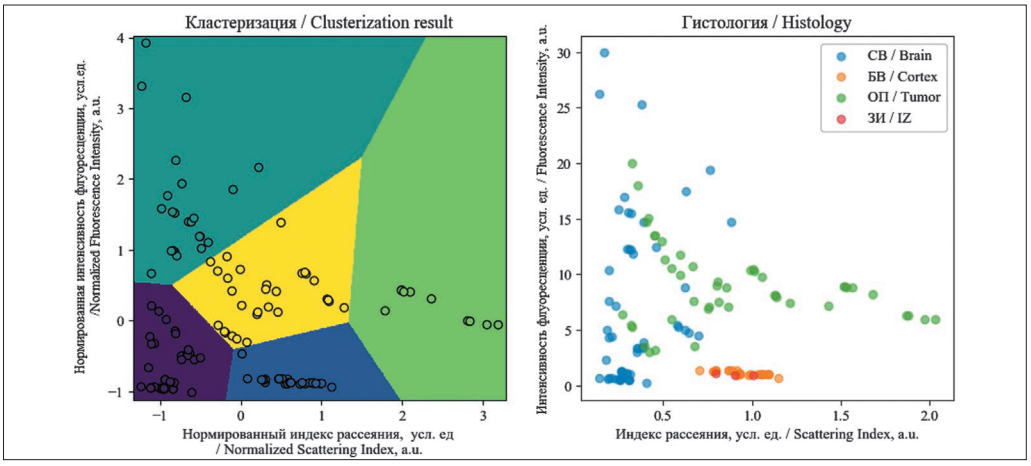

b

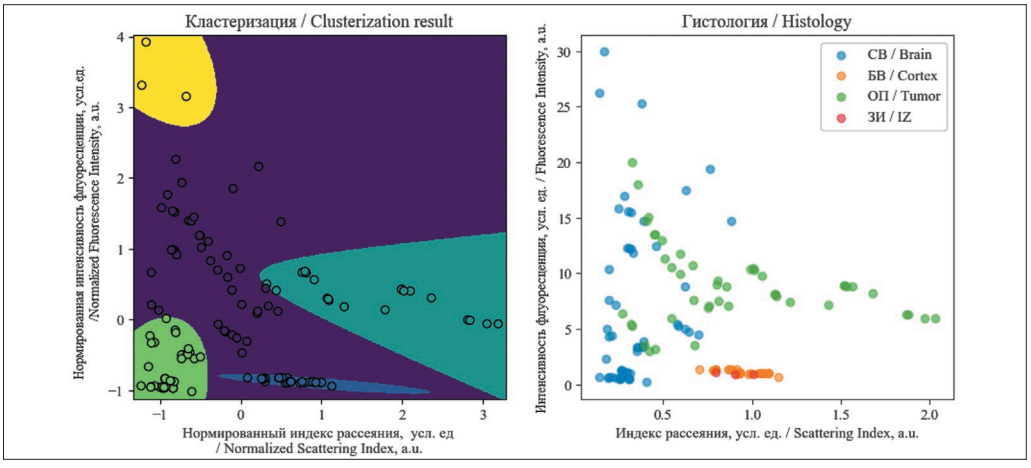

c

Рис. 4. Визуализация результатов пациентов Б.+Г.+С. с применением различных методов кластеризации, в сравнении с реальным распределением объектов (справа), где СВ – серое вещество головного мозга, БВ – белое вещество головного мозга, ОП – опухоль, ЗИ – зона инфильтрации:

a – плотностная кластеризация;
b – кластеризация k-средних;
c – кластеризация EM-алгоритм

Fig. 4. Visualization of clustering results (left) compared to actual distribution (right) for patients B.+G.+S., where IZ – infiltration zone:

a – density-based clustering;
b – k-means clustering;
c – EM-algorithm clustering

Таблица 4
Метрики качества пациентов Б.+Г.+С. на отложенной выборке
Table 4
Quality metrics of held-out set for patients B.+G.+S.

Название Metric	AMI	ARI	Гомогенность Homogeneity	Полнота Completeness	V-мера V-measure	Силуэт Silhouette
ЕМ-алгоритм EM-algorithm	1,0000	1,0000	1,0000	1,0000	1,0000	0,2366
СК SC	1,0000	1,0000	1,0000	1,0000	1,0000	0,2366
ПК DC	0,0191	0,1026	0,0452	0,0544	0,0494	0,2397
k-средних k-means	0,6442	0,8291	0,8058	0,6548	0,7225	0,2366
АК AC	1,0000	1,0000	1,0000	1,0000	1,0000	0,2397

СК – спектральная кластеризация, ПК – плотностная кластеризация, АК – агломеративная кластеризация
SC – spectral clustering, DC – density-based clustering, AC – agglomerative clustering

Таблица 5
Метрики качества предсказаний пациентов на полученных на пациентах Б., Г., С. моделях
Table 5
Quality metrics of patient predictions based on models obtained from patients B., G. and S.

Пациент Patient	Название Metric	AMI	ARI	Гомогенность Homogeneity	Полнота Completeness	V-мера V-measure	Силуэт Silhouette
Д. D.	ЕМ-алгоритм EM-algorithm	1,0000	1,0000	1,0000	1,0000	1,0000	0,1420
	k-средних k-means	0,6860	0,8479	0,8091	0,6976	0,7449	0,1420
Л. L.	ЕМ-алгоритм EM-algorithm	1,0000	1,0000	1,0000	1,0000	1,0000	0,8165
	k-средних k-means	1,0000	1,0000	1,0000	1,0000	1,0000	0,8165
Все All	ЕМ-алгоритм EM-algorithm	1,0000	1,0000	1,0000	1,0000	1,0000	–0,1452
	k-средних k-means	0,5468	0,7529	0,5587	0,7425	0,6376	–0,1452

whereas the k-means method showed a relatively worse result in most cases.

Conclusion

The following most universal models can be distinguished from the visualized models and measured quality metrics: EM-algorithm, k-means method, spectral clustering and agglomerative clustering. However, the last two methods do not provide ready-made models that can evaluate new data, which excludes them in the creation of decision-making assistance systems, but they are suitable for post-processing of the data.

When the number of obtained clusters is greater than the number of the types of labels, it creates practical difficulties in iterating and merging clusters for the evaluation of models. Sensitivity to the sample size can be seen in the quality metrics and the nature of the model boundaries in patient C. and the integrated patients B. + G. + C., who had 12 objects and 41 objects, respectively. In most cases, and with a sufficient sample, almost all algorithms perfectly coped with the task in individual patients, and the method of density clustering, which obtained, on average, poor quality metrics, was found to be special in the identification of objects close in time, which can help in further research.

The drawbacks listed, except the lack of operability on insufficient samples, can be mitigated with the use of other machine learning methods, namely, supervised learning, where the model will be trained on specific answers, which are labels of a class represented by histological findings.

The results of the study of spectroscopic data make it possible to identify correlations between several parameters numerically, with the use of machine learning methods, determined by spectra and histological conclusions about the presence of tissue malignancy signs.

In comparison with the method of statistical data processing presented earlier, the method of intraoperative registration of combined spectra described in the article [8], the sensitivity increased, on average, from 88% to 90%, and the specificity from 82% to 91%.

The results presented in the article were obtained with the use of research equipment of the Core Facilities Center «Technological and Diagnostic Center for the Production, Research and Certification of Micro and Nanostructures» of the Federal State Budgetary Institution of Science A. M. Prokhorov General Physics Institute of the Russian Academy of Sciences.

The study was done with the financial support of the Ministry of Education and Science of the Russian Federation (agreement RFMEFI60717X0183).

REFERENCES

1. De Robles P., Fiest K.M., Frolkis A.D., Pringsheim T., Atta C., St Germaine-Smith C., Day L., Lam D., Jette N. The worldwide incidence and prevalence of primary brain tumors: a systematic review and meta-analysis, *Neuro-Oncology*, 2015, vol. 17(6), pp. 776–783. doi:10.1093/neuonc/nou283
2. Claes A., Idema A.J., Wesseling P. Diffuse glioma growth: a guerilla war, *Acta Neuropathol.*, 2007, vol. 114, pp. 443–458. doi:10.1007/s00401–007–0293–7
3. Sutter M., Eggspuehler A., Grob D., Jeszenszky D., Benini A., Porchet F., Mueller A., Dvorak J. The validity of multimodal intraoperative monitoring (MIOM) in surgery of 109 spine and spinal cord tumors, *Eur Spine J.*, 2007, vol. 16, suppl. 2, pp. 197–208.
4. Savel'eva T.A., Loshchenov V.B., Goryainov S.A., Shishkina L.V., Potapov A.A. A spectroscopic method for simultaneous determination of protoporphyrin IX and hemoglobin in the nerve tissues at intraoperative diagnosis, *Russian Journal of General Chemistry*, 2015, vol. 85, no. 6, pp. 1549–1557.
5. MacQueen J. Some methods for classification and analysis of multivariate observations. In *Proc. 5th Berkeley Symp. on Math. Statistics and Probability*. 1967. pp. 281–297
6. Jianbo S., Jitendra M. Normalized Cuts and Image Segmentation, *IEEE Transactions on PAMI,* 2000, vol. 22(8) , pp. 888–905.
7. Jordan M.I., Xu L. *Convergence results for the EM algorithm to mixtures of experts architectures: Tech. Rep. A.I. Memo No. 1458.* MIT, Cambridge, MA, 1993. 33 p.
8. Potapov A.A., Goriaĭnov S.A., Loshchenov V.B., Savel'eva T.A., Gavrilov A.G., Okhlopkov V.A., Zhukov V.Iu., Zelenkov P.V., Gol'bin D.A., Shurkhaĭ V.A., Shishkina L.V., Grachev P.V., Kholodtsova M.N., Kuz'min S.G., Vorozhtsov G.N., Chumakova A.P. Intraoperative Combined Spectroscopy (Optical Biopsy) of Cerebral Gliomas, *N. N. Burdenko Journal of Neurosurgery*, 2013, vol. 2, pp. 3–10.

ЛИТЕРАТУРА

1. De Robles P., Fiest K.M., Frolkis A.D., et al. The worldwide incidence and prevalence of primary brain tumors: a systematic review and meta-analysis // Neuro-Oncology. – 2015. – Vol. 17(6). – P. 776–783. doi:10.1093/neuonc/nou283
2. Claes A., Idema A.J., Wesseling P. Diffuse glioma growth: a guee rilla war // Acta Neuropathol. – 2007. – Vol. 114. – P. 443–458. doi:10.1007/s00401–007–0293–7
3. Sutter M., Eggspuehler A., Grob D., et al. The validity of multir modal intraoperative monitoring (MIOM) in surgery of 109 spine and spinal cord tumors // Eur Spine J. – 2007. – Vol. 16, Suppl. 2. – P. 197–208.
4. Savel'eva T.A., Loshchenov V.B., Goryainov S.A., et al. A spectrov scopic method for simultaneous determination of protoporphyo rin IX and hemoglobin in the nerve tissues at intraoperative diagł nosis // Russian Journal of General Chemistry. – 2015. – Vol. 85, No. 6. – P. 1549–1557.
5. MacQueen J. Some methods for classification and analysis of mulQ tivariate observations. In Proc. 5th Berkeley Symp. on Math. Statisa tics and Probability. – 1967. – P. 281–297
6. Jianbo S., Jitendra M. Normalized Cuts and Image Segmentation // IEEE Transactions on PAMI. – 2000. – Vol. 22(8). – pp. 888–905.
7. Jordan M.I., Xu L. Convergence results for the EM algorithm to mixtures of experts architectures: Tech. Rep. A.I. Memo No. 1458. – MIT, Cambridge, MA, 1993. – 33 p.
8. Potapov A.A., Goriaĭnov S.A., Loshchenov V.B., et al. Intraoperative Combined Spectroscopy (Optical Biopsy) of Cerebral Gliomas // N. N. Burdenko Journal of Neurosurgery. – 2013. – Vol. 2. – P. 3–10.

COMBINED ENDOSCOPIC TREATMENT OF A PATIENT WITH CANCER OF THE HYPOPHARYNX TO THE UPPER THIRD OF THE ESOPHAGUS WITH COMPLETE CLINICAL AND ENDOSCOPIC EFFECT

Legostaev V.M., Babenkov O.Y., Balitskiy G.V.
Rostov Research Institute of Oncology, Rostov-on-Don, Russia

Abstract

We present a clinical case with a complete endoscopic and clinical effect after endoscopic treatment of a patient with laryngeal cancer involving the upper third of the esophagus. The patient was treated as follows: conformal radiation therapy TFD = 40 gr, targeted chemotherapy using Cetuximab (total dose of 1800 mg). 1.5 months after the end of the treatment, a residual laryngopharyngeal tumor with a spread into the upper third of the esophagus was found during videolaryngoscopy examination. The result of the following histological examination was G2 squamous cell carcinoma. From August 2015 to February 2017, the patient underwent 8 photodynamic therapy sessions in combination with argon plasma coagulation. A control videolaryngoscopy, carried out 1 month after the final session, showed complete tumor regression without cicatricial deformity and narrowing of the esophageal lumen.

Keywords: photodynamic therapy, laryngopharyngeal tumor, fotoditazin.

For citations: Legostaev V.M., Babenkov O.Y., Balitskiy G.V. Combined endoscopic treatment of a patient with cancer of the hypopharynx to the upper third of the esophagus, *Biomedical Photonics*, 2018, vol. 7, no. 4, pp. 35–40. (in Russ.) doi: 10.24931/2413–9432–2018–7–4–35–40.

Contacts: Legostaev V.M., e-mail: oncoendo@aaanet.ru

КОМБИНИРОВАННОЕ ЭНДОСКОПИЧЕСКОЕ ЛЕЧЕНИЕ БОЛЬНОГО РАКОМ ГОРТАНОГЛОТКИ С РАСПРОСТРАНЕНИЕМ НА ВЕРХНЮЮ ТРЕТЬ ПИЩЕВОДА

В.М. Легостаев, О.Ю. Бабенков, Г.В. Балицкий
Ростовский научно-исследовательский онкологический институт, Ростов-на-Дону, Россия

Резюме

Авторы описывают клиническое наблюдение с полным клиническим эффектом после эндоскопического лечения больного раком гортаноглотки, вовлекающим верхнюю треть пищевода. Пациент получал лечение в объеме: конформная лучевая терапия СОД = 40 Гр, таргетная химиотерапия препаратом цетуксимаб, суммарной дозой 1800 мг. Через 1,5 мес после окончания лечения на видео-ларингоскопии была выявлена остаточная опухоль гортаноглотки с распространением на верхнюю треть пищевода. Результат гистологического исследования – плоскоклеточный рак, G2. С августа 2015 по февраль 2017 г. пациенту было проведено 8 курсов фотодинамичец ской терапии в сочетании с аргоноплазменной коагуляцией. На контрольной видеоларингоскопии, выполненной через 1 мес после последнего курса, зарегистрирована полная регрессия опухоли без рубцовой деформации или сужения просвета пищевода.

Ключевые слова: фотодинамическая терапия, опухоль гортаноглотки, фотодитазин.

Для цитирования: Легостаев В.М., Бабенков О.Ю., Балицкий Г.В. Комбинированное эндоскопическое лечение больного раком гортаноглотки с распространением на верхнюю треть пищевода // Biomedical Photonics. – 2018. – Т. 7, № 4. – С. 35–40. doi: 110.24931/2413–9432–2018–7–4–35–40.

Контакты: Легостаев В.М., e-mail: oncoendo@aaanet.ru

Introduction

The laryngopharynx is an anatomically complex area that plays an important role in the body's processes of respiration and digestion, which led to the creation of the term still used in the literature, «decussation of respiratory and digestive tracts» [1]. The prevalence of laryngopharyngeal cancer in the Russian Federation amounted to 11.7 people per 100,000 population in 2016, while the prevalence of esophageal cancer was 9.2 people per

100,000 population. In 2016, laryngopharyngeal cancer at the 1st and 2nd stages was only diagnosed in 3.2% and 13.5% of cases, respectively. Similar indicators for esophageal cancer are significantly higher and amount to 6.2% at the 1st stage and 24.2% at the 2nd stage. This difference can be explained by the fact that dysphagia is manifested much earlier in the case of esophageal cancer compared to laryngopharyngeal cancer due to narrowing of the organ lumen diameter.

The average rate of late-stage diagnosis of laryngopharyngeal cancer in Russia is 43.1%, which is second only to pancreatic cancer (60.5%). These figures are directly correlated to the high mortality rates in the first year after the diagnosis, which are 41.0% and 58.5% for laryngopharyngeal cancer and esophageal cancer, respectively. The search for ways to improve early diagnosis and treatment of laryngopharyngeal cancer and esophageal cancer is a critical task of the modern medicine [2].

In Russia, there is the following trend in the application of different methods of treating malignant tumours: the proportion of surgeries as an independent type of treatment continues to grow. In 2016, it amounted to 54.3% (53.7% in 2015), while the proportion of combination or comprehensive treatment continued to decrease and reached 31.2% (31.3% in 2015), and the proportion of the radiological method alone was 9.8% (10.1% in 2015). The frequency of use of the radiation therapy as an independent type of treatment for laryngopharyngeal cancer amounted to 17.1% in 2016. The combination or comprehensive method was used to treat laryngopharyngeal cancer in 50.8% of cases and esophageal cancer in 49.1% of cases. The rate of using the chemoradiation as an independent type of treatment for laryngopharyngeal cancer was an order of magnitude higher than the one for esophageal cancer and amounted to 15.7% and 1.4%, respectively [3].

In recent years, photodynamic therapy (PDT) has been increasingly used in oncology along with generally accepted methods of treating malignant tumours (surgeries, radiation therapy, medical therapy and their combinations). This treatment method is based on the interaction between a photosensitizer (PS) and light radiation having a wavelength corresponding to the absorption maximum of the applied PS. As a result, photochemical processes are initiated in cells of a malignant tumour and then lead to its death [4].

The development of methods of a direct destructive effect on malignant tumours, such as electroresection, argon plasma coagulation, laser destruction, cryodestruction, radio frequency ablation, significantly expanded the capabilities of surgeons, allowing them to perform cytoreductive surgeries more safely and efficiently. However, none of these methods has a systemic exposure on cancer patients due to significant limitations and contraindications. In contrast to the above mentioned methods of tumour exposure, PDT has a number of advantages, including the following:

1. The direct selective cytotoxic (apoptosis, necrosis) effect on cancer cells that have accumulated a photosensitizer [5–7].
2. The selective damage to the endothelium of blood vessels of a malignant tumour [10, 11].
3. The activation of antitumour immunity due to the selective damage to cell membranes and blood vessels of a malignant tumour [8, 9].
4. PDT is exceedingly rare complicated by perforation, bleeding, fistula and cicatrical strictures formation [10].
5. The latest generation photosensitizers are nontoxic, so the number of PDT courses is unlimited.

Indication for endoscopic PDT:

1. The main organ-preserving method of minimally invasive treatment of malignant tumours at the Tis-T1N0M0 stage for the complete eradication of the tumour.
2. Reopening of respiratory and gastrointestinal tracts.
3. Cytoreduction and stabilisation of the tumour growth.
4. The treatment method chosen for malignant tumours, when the possibilities of other treatment methods are exhausted [10].

According to the Rostov Cancer Research Institute (RCRI), in cases where other methods of antitumour treatment have been exhausted, endoscopic PDT allowed to achieve the full or partial (a decrease in the tumour lesion size by more than 50%) effect in 81.8 % of cases [10].

There are no absolute contraindications to PDT. Relative contraindications to endoscopic PDT are a patient's severe general somatic condition and unstable hemodynamics.

In the department of intraluminal diagnostics of the RCRI, endoscopic photodynamic therapy (PDT) is successfully used in combination with argon plasma coagulation (APC) of malignant tumours of the laryngopharynx and esophagus when surgical or combined treatment is not possible.

The patient K., 59 years old, was referred to the RCRI with a diagnosis of T2N0M0 laryngopharyngeal cancer, the 2nd stage, clinical group 2. The conclusion of the histological examination was moderately differentiated squamous cell cancer without keratinisation, G2. Coexisting diseases: coronary heart disease, stable angina, postinfarction cardiosclerosis (2005), chronic heart failure, myocardiodystrophy, arterial hypertension at the 3rd stage, gastric ulcer in remission.

According to the results of the computed tomography of the chest and abdominal cavity, ultrasound investigation of the neck and abdominal cavity, no data on the presence of regional and distant metastases of the

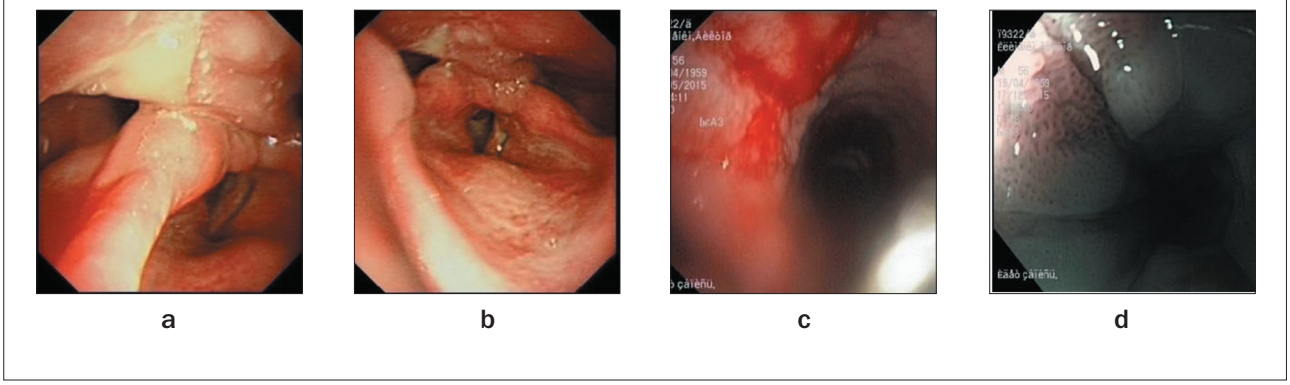

Рис. 1. Результаты видеоларингоскопии и видеоэзофагоскопии:
a, b – резидуальная опухоль задней стенки гортаноглотки;
c – рак устья пищевода с вовлечением его верхней трети (d – осмотр в режиме узкоспектральной эндоскопии)
Fig. 1. Results of videolaryngoscopy and videoesophagoscopy:
a, b – residual tumor of the hypopharynx posterior wall;
c – cancer of the mouth of the esophagus with the involvement of its upper third (d – narrow-band imaging endoscopy examination)

tumour were found. In April 2015, the patient underwent combined chemoradiation therapy (conformal radiation therapy, a single boost dose = 2.4 Gy x 5 fractions per week, a total boost dose = 40 Gy) and targeted chemotherapy with cetuximab at a total dose of 1800 mg.

1.5 months after the treatment, the patient underwent the follow-up videolaryngoscopy (VLS): the mucosa of arytenoid cartilages was swollen and hyperaemic; the tumor infiltrate of 2x2.5 cm in size with a 0.8 cm triangular carcinelcosis was visible on the posterior wall of the laryngopharynx above the arytenoid cartilages. The infiltrate spread over the posterior wall of the pharynx dorsally to the arytenoid cartilages of the larynx, its lower edge was visible in the region of the lower third of the left pyriform sinus (Fig. 1*a, b*).

The patient had no complaints of dysphagia, however, given the outcomes of our previous study confirming the frequent involvement of the esophagus in laryngopharyngeal cancer [11], we decided to perform videoesophagoscopy (VES). When imaged in the narrow band mode, the esophageal mucosa had a pathologically changed relief and an atypical vascular pattern with distinctive signs of neoplasia over the 4 cm circular area in the mouth of the esophagus and right after it (Fig. 1*c, d*). Pathological changes were more severe on the lateral walls of the esophagus. The biopsy was performed. Histological findings: squamous cell cancer, G2.

From April to June 2015, the patient underwent the second stage of the chemoradiation therapy: a single boost dose = 2.4 Gy and 1 Gy x 5 fractions per week (a total boost dose = 60 Gy for the primary site and 50 Gy for the regional lymph nodes), cetuximab at a total dose of 3400 mg. During the follow-up VLS after 1.5 months, a tumour in the laryngopharynx was not detected, but when imaged in the narrow band mode, a residual tumour was found in the mouth of the esophagus and its upper third, which was morphologically confirmed (Fig. 2*a, b*).

Due to the exhausted possibilities of chemoradiation therapy, PDT of the affected area was assigned to the patent at the case conference.

All PDT sessions were conducted 2 hours after IV infusion of the Fotoditazine (VETA-GRAND LLC, Russia, registration licence No. LS 001246 of 18.05.2012) at a dose of 1 mg/kg-BM using the GIF H-180 EXERA II video gastroscope (Olympus, Japan) under general endotracheal anesthesia with artificial lung ventilation. An endoscope with a transparent cap mounted on its distal end was inserted in the laryngopharynx; a quartz light guide with a 2 cm long cylindrical diffuser was inserted through its instrument channel. The light guide was positioned at a

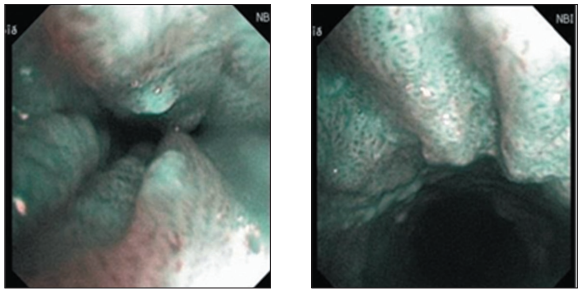

Рис. 2. Остаточная опухоль пищевода (осмотр в узкоспектральном режиме эндоскопии):
a – устье пищевода;
b – верхняя треть пищевода
Fig. 2. Residual esophageal tumor (narrow-band imaging endoscopy examination):
a – the mouth of the esophagus;
b – upper third of the esophagus

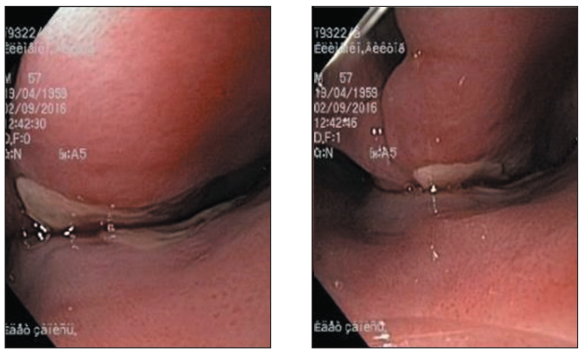

a b

Рис. 3. Результаты видеоларингоскопии, выполненной после 1-го курса ФДТ:
a, b – фаза некроза опухоли гортаноглотки
Fig. 3. Results of videolaryngoscopy performed after the 1st PDT session:
a, b – necrosis phase of the hypopharynx tumor

distance of 1 mm from the tumour. Then the surface of the tumour was irradiated with light using a laser light source (λ=662 nm) (Lakhta-Milon, Russia). The laser irradiation power was 1000 mW, and the energy density was 200 J/cm^2. The irradiation was performed from 4 positions in the laryngopharynx and 6 fields in the esophagus. The time of the irradiation at each point was 4 minutes.

During the first week after PDT, the patient experienced moderate pain in the laryngopharynx, which was managed by taking non-steroidal anti-inflammatory drugs (nimesulide).

10 days after the PDT a follow-up VLS was performed: tumour necrosis with fibrinous deposition, hyperemia and oedema of the surrounding mucosa were detected (Fig. 3*a, b*).

In total, the patient underwent 7 PDT courses under general anesthesia at an interval of 1.5–2 months during the year, while the PDT was conducted three times in combination with argon plasma coagulation of the exophytic area of the tumour (0.8 cm) using the ERBE VIO 300 D electro-surgery unit. 3 weeks after each PDT course, follow-up endoscopic examinations of the laryngopharynx and esophagus were conducted. During each examination, the improvement was observed in the form of a gradual decrease in the size of the residual tumour.

After the 7th course, the full endoscopic effect was achieved in the form of the disappearance of infiltration of the laryngopharyngeal mucosa and the mouth and the upper third of the esophagus (Fig. 4*a, b*).

After 2 months, a rough mucosa site of about 1 cm in diameter with signs of neoplasia was detected in the mouth of the esophagus in a 7 o'clock position with the patient's left lateral position. After the biopsy, histological findings were obtained: squamous cell cancer, G2 (Fig. 5).

The 8th PDT course with APC was conducted. During the follow-up VLS after 1 month, a complete regression

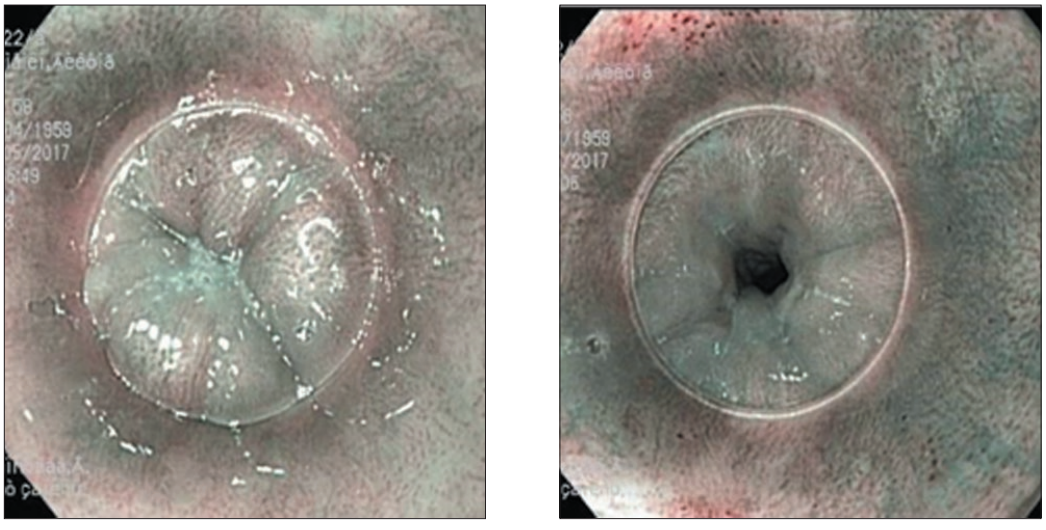

a b

Рис. 4. Результаты узкоспектральной эндоскопии, выполненной после 7 курсов ФДТ:
a – полная регрессия опухолевой инфильтрации устья пищевода;
b – полная регрессия опухолевой инфильтрации верхней трети пищевода
Fig. 4. Results of narrow-band imaging endoscopy performed after 7 PDT sessions:
a – complete regression of tumor infiltration of the mouth of the esophagus;
b – complete regression of tumor infiltration of the upper third of the esophagus

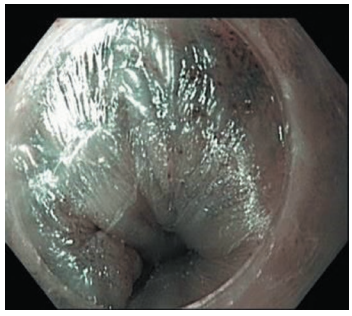

Рис. 5. Рецидив рака пищевода в области его устья (осмотр в режиме NBI)
Fig. 5. Recurrence of cancer in the mouth of the esophagus (NBI examination)

of the tumour without cicatricial deformity and narrowing of the esophageal lumen was detected (Fig. 6). At the moment, the duration of the recurrence-free period is 3 months. The patient has no complaints. Dynamic monitoring is carried out.

Conclusion

The described clinical follow-up indicates that photodynamic therapy of residual laryngopharyngeal and esophageal tumours in combination with argon plasma coagulation shows high efficiency and can be a treatment method chosen for patients with malignant tumours of this localization.

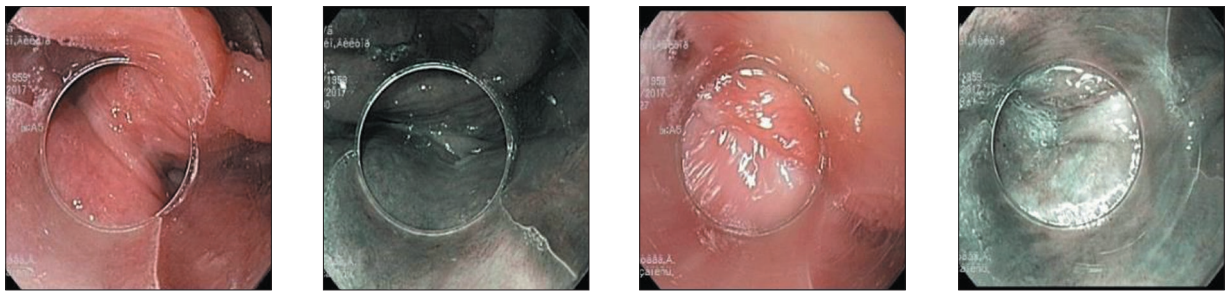

Рис. 6. Результаты контрольной видеоларингоскопии, выполненной после 8 курсов ФДТ (б, г – осмотр в режиме NBI):
a, b – полная регрессия опухолевой инфильтрации гортаноглотки;
c, d – полная регрессия опухоли устья пищевода
Fig. 6. Results of control videolaryngoscopy performed after 8 PDT sessions esophagus (б, г – NBI examination):
a, b – complete regression of the hypopharynx tumor infiltration;
c, d – complete regression of the tumor in the mouth of the esophagus

REFERENCES

1. Paches A.I., Ol'shanskij V.O., Lyubaev V.L., Tuok T.H. *Zlokachestvennye opuholi polosti rta, glotki i gortani* [Malignant tumors of oral cavity, pharynx and larynx]. Moscow, Meditsina Publ., 1988. 304 p.
2. *Rukovodstvo po onkologii* [Guide to Oncology] by eds V.I. Chissov, S.L. Dar'yalova. Moscow, OOO "Medicinskoe informacionnoe agentstvo" Publ., 2008. 904 p.
3. *Sostoyanie onkologicheskoj pomoshchi naseleniyu Rossii v 2016 godu* [Evaluation of the oncological help to the population of Russia in 2016] by eds Kaprin A.D., Starinskiy V.V. Moscow, MNIOI im. P.A. Gertsena – filial FGBU «NMIRC» Minzdrava Rossii Publ., 2017. 236 p.
4. Akopov A.L., Kazakov N.V., Rusanov A.A., Karlson A. The mechanisms of photodynamic action for treating of cancer patients, *Photodynamic therapy and photodyagnosis*, 2015, vol. 4, no. 2,, pp. 9–16. (in Russian) https://doi.org/10.24931/2413–9432–2015–4–2–9–16
5. Agarwal R., Korman N.J., Mohan R.R., Feyes D.K., Jawed S., Zaim M.T., Mukhtar H. Apoptosis is an early event during phthalocyanine photodynamic therapy-induced ablation of chemically induced squamous papillomas in mouse skin, *J. Photochem Photobiol*, 1996, vol. 63, no. 4, pp. 547–552.
6. Kerr J.F., Wyllie A.H., Currie A.R. Apoptosis: a basic biological phenomenon with wide-ranging implications in tissue kinetics, *Brit. J. Cancer*, 1972, vol. 26, pp. 239–257.

ЛИТЕРАТУРА

1. Пачес А.И., Ольшанский В.О., Любаев В.Л., Туок Т.Х. Злокачественные опухоли полости рта, глотки и гортани. – М.: Медицина, 1988. – 304 с.
2. Руководство по онкологии / под ред. В.И. Чиссова, С.Л. Дарьяловой. – М.: ООО «Медицинское информационное агентство», 2008. – 904 с.
3. Состояние онкологической помощи населению России в 2016 году / под ред. А.Д. Каприна, В.В. Старинского. – М.: МНИОИ им. П.А. Герцена – филиал ФГБУ «НМИРЦ» Минздрава России, 2017. – 236 с.
4. Акопов А.Л., Казаков Н.В., Русанов А.А., Карлсон А. Механизмы фотодинамического воздействия при лечении онкологических больных // Фотодинамическая терапия и фотодиагностика. – 2015. – Т. 4, № 2. – С. 9–16. https://doi.org/10.24931/2413–9432–2015–4–2–9–16
5. Agarwal R., Korman N.J., Mohan R.R., et al. Apoptosis is an early event during phthalocyanine photodynamic therapy-induced ablation of chemically induced squamous papillomas in mouse skin // J. Photochem Photobiol. – 1996. – Vol. 63, No. 4. – P. 547–552.
6. Kerr J.F., Wyllie A.H., Currie A.R. Apoptosis: a basic biological phenomenon with wide-ranging implications in tissue kinetics // Brit. J. Cancer. – 1972. – Vol. 26. – P. 239–257.

7. Oleinick N. L., Morris L., Varnes M. E. The peripheral benzodiazepine photosensitizer Pc4, *J. Photochem. and Photobiol.,* 2002, vol. 75(6), pp. 652–661.
8. Krosl G., Korbelik M. Potentiation of photodynamic therapy by immunotherapy: the effect of schizophyllan (SPG), *Cancer Lett.*, 1994, vol. 84, pp. 43–49.
9. Coutier S., Bezdetnaya L., Marchal S., Melnikova V., Belitchenko I., Merlin J.L., Guillemin F. Foscan (mTHPC) photosensitized macrophage activation: enhancement of phagocytosis, nitric oxide release and tumour necrosis factor-alpha-mediated cytolytic activity, *Br. J. Cancer*, 1999, Vol. 81, pp. 37–42.
10. Legostaev V.M., Babenkov O. Yu., Maldonado G. M., Islamova E.F., Balitsky G.V. Endoscopic photodynamic therapy of malignant tumors as a method of choice with exhausted possibilities of other methods of treatment in *Materials XLIX International Scientific and Practical Conference "Application of Lasers in Medicine and Biology" and "2nd Gamaleia's Readings"*. Kharkiv, 2018. 42–47 p.
11. Kravchenko A.B., Legostaev V.M., Babenkov O.Yu., Nosov V.A. Skriningovaya ehzofagoskopiya u patsientov, napravlennykh na endoskopicheskoe issledovanie dyhatel'nyh putej [Screening esophagoscopy in patients aimed at endoscopic examination of the respiratory tract] in *Vserossijskaya molodezhnaya konferenciya «Aktualnye voprosy eksperimentalnoi i klinicheskoj onkologii. Sbornik tezisov*. Rostov-na-Donu, 2016. p. 60

7. Oleinick N.L., Morris L., Varnes M.E. The peripheral benzodiazepine photosensitizer Pc4 // J. Photochem. and Photobiol. – 2002. – Vol.75(6). – P. 652–661.
8. Krosl G., Korbelik M. Potentiation of photodynamic therapy by immunotherapy: the effect of schizophyllan (SPG) // Cancer Lett. – 1994. – Vol. 84. – P. 43–49.
9. Coutier S., Bezdetnaya L., Marchal S., et al. Foscan (mTHPC) photosensitized macrophage activation: enhancement of phagocytosis, nitric oxide release and tumour necrosis factor-alpha-mediated cytolytic activity // Br. J. Cancer. – 1999. – Vol. 81. – P. 37–42.
10. Legostaev V.M., Babenkov O.Yu., Maldonado G.M., et al. Endoscopic photodynamic therapy of malignant tumors as a method of choice with exhausted possibilities of other methods of treatment / Materials XLIX International Scientific and Practical Conference "Application of Lasers in Medicine and Biology" and "2nd Gamaleia's Readings". – Kharkiv, 2018. – 42–47 p.
11. Кравченко А.Б., Легостаев В.М., Бабенков О.Ю., Носов В.А. Скрининговая эзофагоскопия у пациентов, направленных на эндоскопическое исследование дыхательных путей / Всероссийская молодежная конференция «Актуальные вопросы экспериментальной и клинической онкологии». Сборник тезисов. – Ростов-на-Дону, 2016. – С. 60.